STRESS CONCENTRATIONS IN FILAMENT-STIFFENED SHEETS

by

WILBUR BRYAN FICHTER

A thesis submitted to the Graduate Faculty of
North Carolina State University at Raleigh
in partial fulfillment of the
requirements for the Degree of
Doctor of Philosophy

DEPARTMENT OF ENGINEERING MECHANICS

RALEIGH

1969

APPROVED BY:

Chairman of Advisory Committee

ABSTRACT

FICHTER, WILBUR BRYAN. Stress Concentrations in Filament-Stiffened Sheets. (Under the direction of EDWARD DEWITT GURLEY).

An influence-function technique is employed to analyze the stresses and deformations due to flaws in an idealized composite material composed of parallel, equally spaced, tension-carrying filaments embedded in a shear-carrying matrix. Static tensile stress concentration factors are obtained for the cases of two equal-length transverse collinear cuts across various numbers of filaments, and for the case of a periodic array of transverse collinear cuts. In addition, a static shear stress concentration factor is obtained for a single cut across an arbitrary number of consecutive filaments. Dynamic stress concentration factors are obtained for two cases in which two collinear cuts are suddenly introduced into a stretched filamentary sheet. Matrix shear loads are investigated and their variation in the longitudinal direction is studied for several cases involving single and double cuts. In addition, loads in broken filaments are calculated for some single-cut cases, and their implications for an existing statistical tensile failure analysis for composite materials are briefly discussed.

In the case of two collinear cuts it is found that interaction between the two cuts is significant only when the distance between the cuts is no greater than the cut length and, hence, that more widely spaced cuts may, for all practical purposes, be treated as isolated cuts. The interaction between closely spaced cuts, however, is pronounced. It is found that two closely spaced cuts can cause higher stress concentrations than a single cut across a comparable total

number of filaments. This result suggests that a design criterion based on the residual strength of a composite weakened by a single cut of prescribed length can be unconservative, even though only cuts of lesser length are present.

The stress concentration factors for a periodic array of collinear cuts, which for the present model are equivalent to the stress concentration factors for a transverse cut in a strip of filament-stiffened material, are found to agree closely with results of an earlier approximate analysis, except for cut lengths approaching the width of the strip. This indicates that in the practical range of interest of the cut-length to strip-width ratio, the approximate stress concentration factor is sufficiently accurate for engineering purposes.

The matrix shear stress concentration factor for a single cut of arbitrary length is seen to increase with cut length somewhat more rapidly than the tensile stress concentration factor, particularly for the shorter cuts. This suggests that some filamentary composites might be primarily susceptible to tensile failure when weakened by small flaws, but might be more susceptible to matrix shear failure when larger flaws are present.

Results of limited calculations of filament dynamic stress concentration factors for two collinear cuts are in agreement with earlier results for a single cut, and support the previous conclusion that dynamic effects are of secondary importance for the type of model investigated.

Calculations of the longitudinal variation of matrix shear forces show that they decay less rapidly with increasing cut length. Broken filaments are seen to recover load less rapidly with greater cut length, a result which suggests that tensile failure analyses for imperfect composites, depending strongly on the ineffective length of broken filaments, should account for the variation of ineffective length with flaw size, rather than employ a single value of ineffective length regardless of the distribution of initial imperfections.

BIOGRAPHY

The author was born July 19, 1935, in Kinston, North Carolina. He attended public schools in Kinston, graduating from Grainger High School in 1953.

He received the Bachelor of Science degree with a major in mathematics from Wake Forest College in 1957. In July 1957, he accepted a position with the National Advisory Committee for Aeronautics (now the National Aeronautics and Space Administration) at Langley Research Center, Hampton, Virginia, where he is presently employed. In 1966, he received the Master of Science degree in engineering mechanics from Virginia Polytechnic Institute.

The author married Miss Ann Bowles in 1958, and they have two children, Bryan Gregory, eight years old; and Lee Ann, six years old.

ACKNOWLEDGEMENTS

The author wishes to express his appreciation to Professor E. D. Gurley, Chairman of his Advisory Committee, for his counsel and assistance in the preparation of this work. Appreciation is also extended to Professors W. J. Harrington, R. A. Douglas, M. H. Clayton, and C. J. Maday for their constructive suggestions.

Special gratitude is extended to two members of the Structures Research Division, NASA-Langley Research Center: Mrs. Nancy P. Sykes for her assistance with the mathematical calculations, and Mrs. Ruth A. Pokorski for her typing of the initial drafts.

Finally, the author expresses his deepest appreciation to his wife, Ann, and his children for their patience and sacrifice during the course of his studies.

TABLE OF CONTENTS

Page

LIST OF TABLES

LIST OF FIGURES

INTRODUCTION

Composite materials are finding increasingly wide application in aerospace structures. For example, many solid-propellant rocket motor cases are constructed by winding resin-coated glass filaments on a mandrel. Coated fabrics, because of their great flexibility, have been used in applications requiring the temporary packaging of large, low-density structures into small storage volumes Currently, much effort is being applied to the development of lightweight composite materials, which typically are composed of high-modulus filaments embedded in plastics or metals of relatively low density and modulus.

The rational design of a structure requires knowledge of the stresses which it is likely to experience. However, because of their inhomogeneity, composite structures often do not lend themselves to representation by tractable mathematical models. For example, the walls of filament-wound rocket motor cases are constructed of numerous layers of windings, with the winding direction varying from one group of layers to another. A structure of such complexity presents formidable analytical difficulties. However, if attention is focused on a single layer of composite material, it is possible to obtain analytical results which may be applicable ultimately to more complex arrangements.

The problem of stress concentration in aerospace structures is one of continuing importance. In reference 4, a stress concentration problem for a plane of parallel, equally spaced filaments embedded in

a matrix was formulated and solved by Hedgepeth. The principal results of the analysis were the static and dynamic stress concentration factors caused by a single cut across a number of adjacent filaments. In reference 5, this analysis was extended by Hedgepeth and Van Dyke to problems involving some special two-dimensional distributions of parallel filaments.

In this thesis, the analysis of reference 4 is extended to the cases of two collinear cuts and of periodic collinear cuts of equal length. Also, the single-cut problem of reference 4 is re-examined for the purpose of more fully exploiting the potential of the model for the study of some composite materials. Specifically, matrix shear forces, and the decay of matrix shear forces and filament tensile forces with axial distance from the cut are studied. In addition, an expression for maximum shear force, analogous to the filament stress concentration factor, is determined for the case of a single cut.

In the case of a double cut, static stress concentration factors are computed and compared with some related single-cut results. In addition, dynamic stress concentration factors are calculated for two of the simplest double-cut cases.

For the problem of periodic collinear cuts, which is related to the problem of a finite-width sheet weakened by a central cut, static stress concentration factors are calculated for various combinations of cut length and distance between cuts, and are compared with results of an approximate analysis for an isotropic elastic sheet

REVIEW OF LITERATURE

An extensive survey of research in composite materials, with particular emphasis on fibrous or filamentary composites, is contained in reference 6, where numerous additional references are cited. Particularly relevant to the present work are references 4 and 5.

In reference 4, an analysis is presented of the stress concentration around a single straight cut across an arbitrary number of filaments in an idealized composite composed of a single infinite layer of parallel, equally spaced, tension-carrying filaments embedded in a shear-carrying matrix. A closed-form expression was obtained for the stress concentration factor (defined as the ratio of the highest load in an unbroken filament to the far-field applied load) as a function of the number of broken filaments. This result was substantiated experimentally by Zender and Deaton in reference 9. In reference 4, other phenomena of interest, such as matrix shear forces, and the variation of filament and matrix loads in the filament direction, were not investigated.

In reference 5, the influence function technique introduced in reference 4 was extended to the problem of stress concentration in a composite material composed of two-dimensional arrays of filaments embedded in a shear-carrying matrix. Because of the difficulty of obtaining closed-form inversions for various transformed quantities, extensive numerical computation was required. It was found that, in general, the breaking of a given number of neighboring filaments causes

greater stress concentration in the single layer than in the two-dimensional array. An additional analysis of a single layer, in which the matrix material around a single broken filament was assumed to undergo ideal plastic deformation over a portion of the filament length, indicated that the inclusion of matrix plasticity mitigates the filament stress concentration effect predicted by the elastic analysis. However, it appears that the results are too limited for sweeping conclusions to be drawn regarding the effects of plastic deformation in an imperfect filamentary composite. Experimental verification of the results of reference 5, in view of the necessarily more complicated nature of the mathematical models, is likely to prove much more difficult than was the case with the single-layer elastic model

LIST OF SYMBOLS

d	filament spacing
d_f	filament diameter
EA	extensional stiffness of a filament
E_n	Weber function
Gh	shear stiffness of the matrix
h	effective thickness of the matrix
I_n	modified Bessel function of the first kind
i,k,m,n,q,r,s	integers
J_n	Bessel function of the first kind
K	filament stress concentration factor
L_n	modified Struve function
N_n	load in n^{th} filament for influence-function solution (L_n of reference 4)
p	force applied to each filament at infinity
p_n	load in n^{th} filament
P_n	dimensionless load in n^{th} filament, p_n/p
S_{max}	maximum dimensionless matrix shear force
S_n	dimensionless matrix shear force between n^{th} and $(n+1)^{th}$ filaments, $\frac{s_n}{p}\sqrt{\frac{EAd}{Gh}}$
s_n	matrix shear force per unit length between n^{th} and $(n+1)^{th}$ filaments
t	time
u_n	displacement of n^{th} filament

U_n	dimensionless displacement of n^{th} filament, $\frac{u_n}{p}\sqrt{\frac{EAGh}{d}}$
V_n	displacement of n^{th} filament for influence-function solution
x	coordinate parallel to filaments
z	complex variable
γ	mass per unit length associated with a filament
ξ	dimensionless coordinate parallel to filaments, $x\sqrt{\frac{Gh}{EAd}}$
θ	variable of integration
τ	dimensionless time, $t\sqrt{\frac{Gh}{\gamma d}}$
ζ	transform variable

GOVERNING EQUATIONS

As far as is practical the notation employed in reference 4 is retained in the present analysis. The configuration is shown in figure 1, along with the coordinate system and some notation. The analytical model is one which is commonly used in "shear-lag" analyses. It is composed of an infinite single layer of parallel tension-carrying members (filament) embedded in a matrix which carries only shear. The filaments are separated by a constant distance d and are numbered from $-\infty$ to ∞ from the bottom upward. The coordinate along the filaments is x and the displacement of the n^{th} filament at location x is $u_n(x,t)$. The force in the n^{th} filament is denoted by $p_n(x,t)$ and is given in terms of u_n by

$$p_n = EA \frac{\partial u_n}{\partial x} \tag{1}$$

where EA is the extensional stiffness of the filament. The shear force per unit length between the n^{th} and $(n+1)^{th}$ filaments is defined here by $s_n = \frac{Gh}{d}(u_{n+1} - u_n)$. Conservation of momentum of the n^{th} filament then requires

$$\frac{\partial p_n}{\partial x} + s_n - s_{n-1} = \gamma \frac{\partial^2 u_n}{\partial t^2}$$

where the assumption has been made that the mass per unit length γ associated with the n^{th} filament is concentrated at that filament. In terms of displacements, the equation of motion becomes

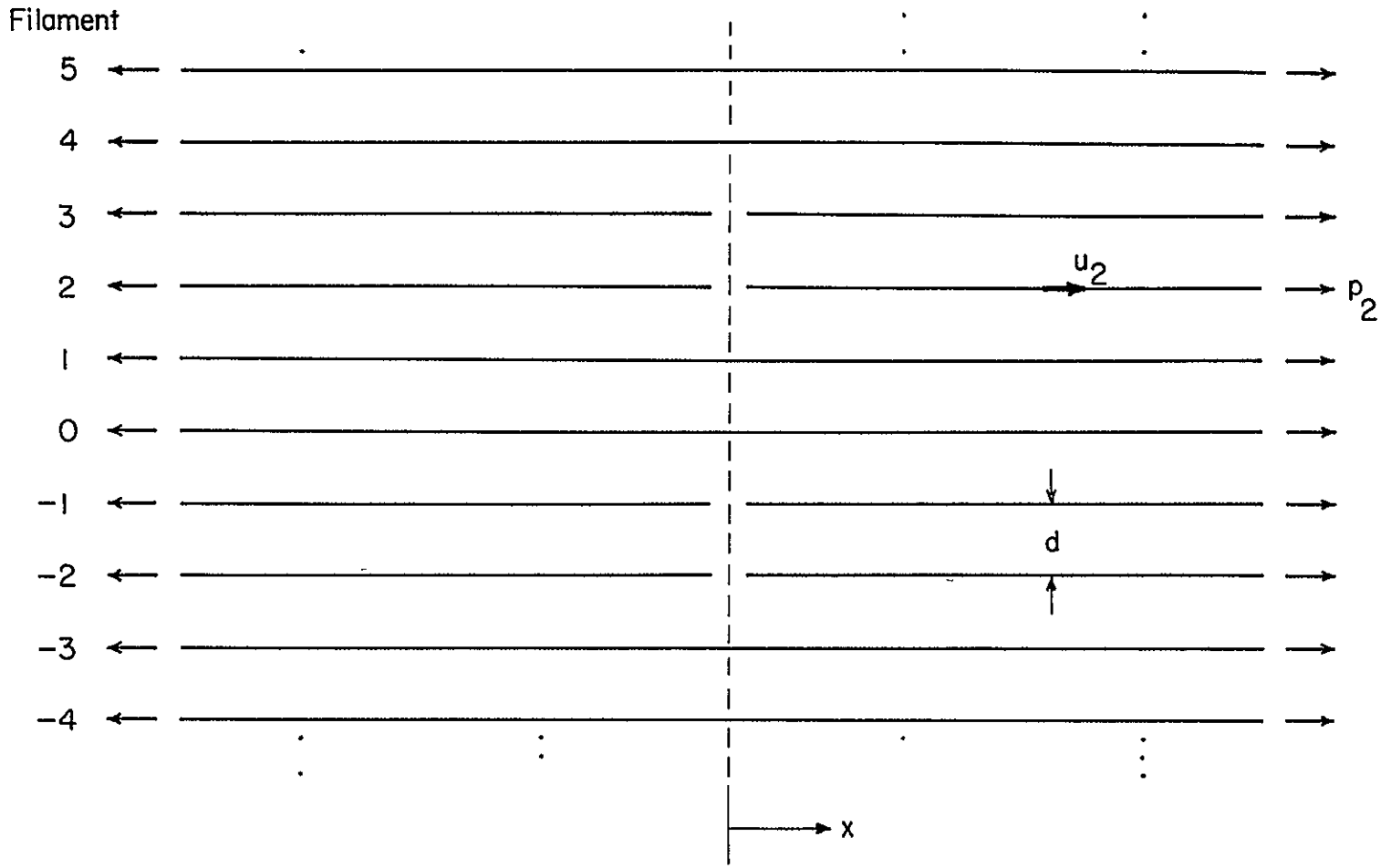

Figure 1. Coordinate and notation systems

$$EA \frac{\partial^2 u_n}{\partial x^2} + \frac{Gh}{d}(u_{n+1} - 2u_n + u_{n-1}) = \gamma \frac{\partial^2 u_n}{\partial t^2} \tag{2}$$

In figure 1, filaments -2, -1, 2 and 3 are shown broken at $x = 0$, with the remaining filaments intact. In general, for two collinear cuts (at $x = 0$) through q and s filaments, let $-(m + q) \leqq n \leqq -(m + 1)$ and $r + 1 \leqq n \leqq r + s$, respectively, denote the broken filaments, the two cuts being separated by $r + m + 1$ intact filaments. Then the boundary conditions are

$$u_n(0,t) = 0, \quad -m \leqq n \leqq r, \quad -(m + q + 1) \geqq n, \quad n \geqq r + s + 1 \tag{3}$$

and

$$p_n(0,t) = 0, \quad -(m + q) \leqq n \leqq -(m + 1), \quad r + 1 \leqq n \leqq r + s$$

For x large, the force in each filament approaches the uniform applied force, denoted by p; that is

$$p_n(\pm\infty,t) = p \tag{4}$$

For the time-dependent problem, the following initial conditions are required:

$$p_n(x,0) = p$$

$$\frac{\partial u_n}{\partial t}(x,0) = 0 \tag{5}$$

For convenience, let

$$
\begin{aligned}
p_n &= pP_n \\
u_n &= p\sqrt{\frac{d}{EAGh}}\, U_n \\
s_n &= p\sqrt{\frac{Gh}{EAd}}\, S_n \\
x &= \sqrt{\frac{EAd}{Gh}}\, \xi \\
t &= \sqrt{\frac{\gamma d}{Gh}}\, \tau
\end{aligned}
\tag{6}
$$

Then the equilibrium equation becomes

$$
\frac{\partial^2 U_n}{\partial \xi^2} + U_{n+1} - 2U_n + U_{n-1} = \frac{\partial^2 U_n}{\partial \tau^2} \tag{7}
$$

with boundary conditions

$$
\begin{aligned}
&U_n(0,\tau) = 0, \quad -m \leqq n \leqq r, \quad -(m+q+1) \geqq n, \quad n \geqq r+s+1 \\
&P_n(0,\tau) = 0, \quad -(m+q) \leqq n \leqq -(m+1), \quad r+1 \leqq n \leqq r+s \\
&P_n(\pm\infty,\tau) = 1
\end{aligned}
\tag{8}
$$

and initial conditions

$$P_n(\xi,0) = 1$$

$$\frac{\partial U_n}{\partial \tau}(\xi,0) = 0 \tag{9}$$

The dimensionless forces and displacements are related by

$$P_n(\xi,\tau) = \frac{\partial U_n}{\partial \xi}$$

and (10)

$$S_n = U_{n+1} - U_n$$

SOLUTIONS

Stress Concentration Factors

The boundary value problem for static loading is defined by equation (7) with the right hand side set equal to zero, and boundary conditions (8). The solution is complicated by the fact that the boundary conditions at $\xi = 0$ are mixed. This difficulty was overcome in reference 4 by use of an influence function technique. For a thorough discussion of this technique, the reader is referred to reference 4. The influence functions $V_n(\xi)$ and $N_n(\xi) = dV_n(\xi)/d\xi$ are, respectively, the nondimensional displacement and force in the n^{th} filament when the filament sheet is completely cut along $\xi = 0$ and the zeroth filament is displaced axially a unit amount at $\xi = 0$ while all other filaments are held fixed at $\xi = 0$. In terms of $V_n(\xi)$ and $N_n(\xi)$, the dimensionless force and displacement are given by

$$\begin{aligned} P_n(\xi) &= 1 + \sum_{i=-\infty}^{\infty} N_{n-i}(\xi)U_i(0) \\ U_n(\xi) &= \xi + \sum_{i=-\infty}^{\infty} V_{n-i}(\xi)U_i(0) \end{aligned} \tag{11}$$

In reference 4, $V_n(\xi)$ was found to be

$$V_n(\xi) = \frac{1}{\pi} \int_0^{\pi} \cos n\theta e^{-2\xi \sin \theta/2} d\theta \tag{12}$$

Application of boundary conditions (8) to equations (11) yields first

$$P_n(\xi) = 1 + \sum_{i=-(m+q)}^{-(m+1)} N_{n-i}(\xi)U_i(0) + \sum_{i=r+1}^{r+s} N_{n-i}(\xi)U_i(0)$$

$$U_n(\xi) = \xi + \sum_{i=-(m+q)}^{-(m+1)} V_{n-i}(\xi)U_i(0) + \sum_{i=r+1}^{r+s} V_{n-i}(\xi)U_i(0) \tag{13}$$

since $U_i(0) = 0$ for other values of i, and second

$$0 = 1 + \sum_{i=-(m+q)}^{-(m+1)} N_{n-i}(0)U_i(0) + \sum_{i=r+1}^{r+s} N_{n-i}(0)U_i(0), \qquad \begin{matrix} -(m+q) \leq n \leq -(m+1) \\ \text{and} \\ r+1 \leq n \leq r+s \end{matrix} \tag{14}$$

which expresses the condition of zero load on the ends of the broken filaments.

Equations (14) constitute a set of $q + s$ linear algebraic equations in the $q + s$ unknowns, $U_n(0)$. Their solution set can be substituted into equations (13) to obtain expressions for load and displacement in any filament. However, before this can be done, the integral representation of the influence functions, $V_n(\xi)$ and $N_n(\xi)$ must be evaluated. Only $N_n(0) = dV_n(0)/d\xi$ was evaluated in reference 4 because the computation of stress concentration factors, which was the main purpose of that investigation, does not require the evaluation of the influence functions for non-zero values of ξ. Equation (12) can also be written as

$$V_n(\xi) = \frac{1}{\pi} \int_0^{\pi} \cos 2n\theta e^{-2\xi \sin\theta} d\theta \tag{15}$$

Integration of this expression has been carried out in Appendix A. The result is

$$V_n(\xi) = (-1)^n \left[I_{2n}(2\xi) - L_{2n}(2\xi) - \frac{1}{\pi} \sum_{k=0}^{n-1} (-1)^k \frac{\Gamma\left(k + \frac{1}{2}\right) \xi^{2n-2k-1}}{\Gamma\left(2n + \frac{1}{2} - k\right)} \right], \quad n \geq 0 \tag{16}$$

in which I_{2n} is the modified Bessel function of the first kind, L_{2n} is the modified Struve function (see reference 1), and the finite sum must be taken to be zero for $n = 0$. A similar expression for $V_n(\xi)$ can be derived for $n < 0$; this is not necessary, however, since it can be seen from equation (15) that $V_{-n}(\xi) = V_n(\xi)$. Differentiation of equation (16) yields

$$N_n(\xi) = (-1)^n \left[I_{2n+1}(2\xi) + I_{2n-1}(2\xi) - \left\{ L_{2n+1}(2\xi) + L_{2n-1}(2\xi) + \frac{\xi^{2n}}{\pi^{1/2}\, \Gamma\left(2n + \frac{3}{2}\right)} \right\} - \frac{1}{\pi} \sum_{k=0}^{n-1} (-1)^k \frac{(2n - 2k - 1)\Gamma\left(k + \frac{1}{2}\right) \xi^{2n-2k-2}}{\Gamma\left(2n + \frac{1}{2} - k\right)} \right],$$

$$n \geq 0 \tag{17}$$

in which the finite sum again is to be omitted for $n = 0$. From equation (17) it is found that

$$N_n(0) = \frac{4}{\pi(4n^2 - 1)} \tag{18}$$

in agreement with reference 4.

With substitution of the appropriate values from equation (18), equations (14), which are merely linear algebraic equations for the displacements of the ends of the broken filaments, can be solved. Then the solutions to equations (14), along with the influence functions given by equations (16) and (17), can be substituted into equations (13) to obtain the load and displacement of any filament in the sheet.

Tensile stress concentration factors for two collinear cuts.- In the case of a single cut in a filamentary sheet, the stress concentration factor depends only upon the number of consecutive filaments traversed by the cut. In reference 4, the stress concentration factor for a cut across n consecutive filaments was found to be

$$K_n = \frac{4 \cdot 6 \cdot 8 \cdots (2n + 2)}{3 \cdot 5 \cdot 7 \cdots (2n + 1)}, \quad n = 1,2,3,\ldots \tag{19}$$

where K_n is the ratio of the maximum load in either of the two intact filaments directly adjacent to the cut, to the load at infinity.

In the case of two cuts, two additional parameters appear: (1) the number of broken filaments in the second cut, and (2) the number of intact filaments separating the two cuts. In general, each cut may sever any number of filaments and any number of intact filaments may separate the two cuts. Hence the general case of two collinear cuts is

without symmetry, and calculations covering reasonably wide variations of the three pertinent parameters would entail a considerable computational effort. However, if the problem is simplified by requiring the cuts to be of equal length, then the most essential features of the two-cut problem are retained while the computational effort is greatly reduced through consideration of the resulting symmetries.

In what follows, then, it is assumed that the two cuts traverse the same number of filaments. In the analysis of this reduced problem one of two cases arises, depending on whether the number of intact filaments between the cuts (henceforth called "interior filaments") is even or odd. The analysis of these two cases is presented in Appendix B.

The double-cut stress concentration factor $K_{n,m}$ is defined as the ratio of the greatest load in the most highly stressed unbroken filament to the load at infinity, for two collinear cuts, each across n filaments, and separated by m interior filaments. For an odd number $(2r + 1)$ of interior filaments, the stress concentration factor for two collinear cuts, each across n filaments is found in Appendix B to be

$$K_{n,2r+1} = 1 + \sum_{i=r+1}^{r+n} \left\{ N_{r+1}(0) + N_{r-1}(0) \right\} U_i(0) \qquad (20)$$

where each $U_1(0)$ is calculated from equations (B4). For an even number $(2r)$ of interior filaments,

$$K_{n,2r} = 1 + \sum_{i=r}^{r+n-1} \left\{ N_{r+i}(0) + N_{r-i-1}(0) \right\} U_1(0) \qquad (21)$$

where each $U_i(0)$ is calculated from equations (B10).

The stress concentration factors, given by equations (20) and (21), have been computed for two equal-length collinear cuts, each traversing from one to eight filaments and separated by intact filaments ranging in number from one to 16. The results are presented in Table 1, and are plotted in figure 2 for the various values of n, the number of filaments severed by each cut. Although the curves are meaningful only for integral values of n, they are plotted as continuous curves for illustrative purposes. Also shown in figure 2 are the single-cut stress concentration factors K_n, which are the asymptotic values of $K_{n,m}$ for large m.

As can be seen in figure 2, the interaction between cuts is essentially a local phenomenon, being confined to separation distances (values of m) on the order of the cut length. The results indicate that cuts which are separated by distances greater than their length may, for all practical purposes, be treated as isolated cuts.

For closely spaced cuts (small m), however, the interaction is pronounced. Hence, the values of $K_{n,m}$ for small m are of particular interest, since they are associated with states of high stress concentration. In order to present a comparison of the severities of single and double cuts, the stress concentration factors for two cuts of length n separated by one and two intact filaments, $K_{n,1}$ and $K_{n,2}$,

Table 1. Filament stress concentration factors for two collinear cuts of equal length

No. of filaments between cuts, m	No. of filaments in each cut, n							
	1	2	3	4	5	6	7	8
1	1.714	2.359	2.964	3.543	4.102	4.646	5.177	5.698
2	1.412	1.788	2.142	2.481	2.808	3.126	3.436	3.740
3	1.368	1.690	1.989	2.272	2.543	2.805	3.061	3.310
4	1.353	1.654	1.928	2.185	2.430	2.666	2.895	3.118
5	1.346	1.636	1.897	2.140	2.370	2.590	2.803	3.009
6	1.342	1.626	1.879	2.113	2.333	2.542	2.745	2.940
7	1.340	1.620	1.867	2.095	2.308	2.510	2.705	2.893
8	1.338	1.615	1.859	2.082	2.290	2.488	2.677	2.859
9		1.612	1.854	2.073	2.278	2.471	2.655	2.833
10			1.849	2.066	2.268	2.458	2.639	2.813
11			1.846	2 061	2.261	2.448	2.626	2.798
12				2.057	2.255	2.440	2.616	2.785
13				2.054	2.250	2.434	2.608	2.775
14					2.246	2.428	2.601	2 766
15					2.243	2.424	2.595	2.759
16						2.420	2.590	2.753

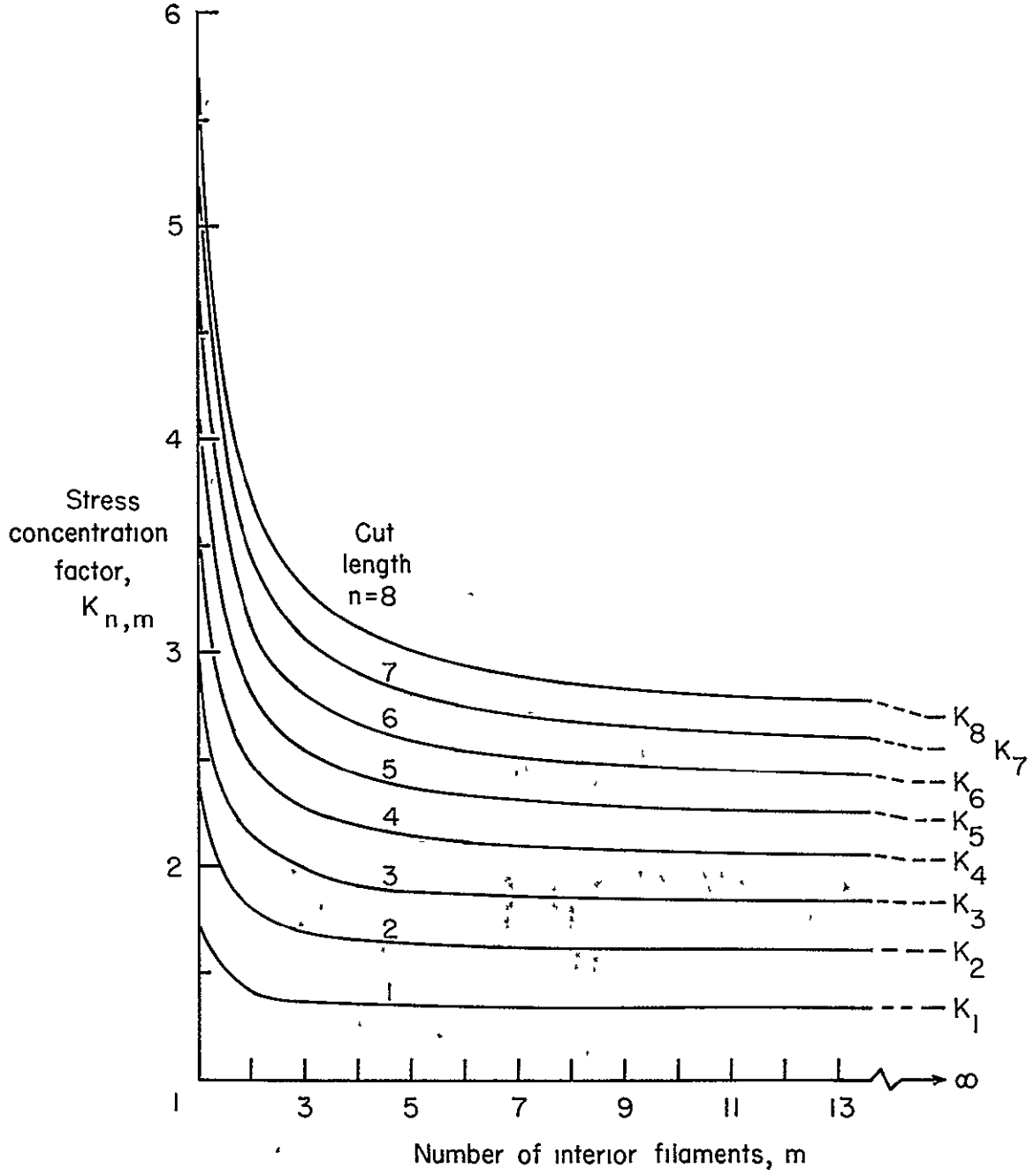

Figure 2. Filament stress concentration factors for two equal-length collinear cuts

are compared with K_{2n}, K_{2n+1}, and K_{2n+2} in figure 3. These particular values of the single-cut stress concentration factor have been chosen because they represent either the same total number (2n) of broken filaments as does $K_{n,m}$, or the number (2n + 1 or 2n + 2) which would be broken if the pair of cuts separated by one or two intact filaments, characterized by $K_{n,1}$ or $K_{n,2}$, were to coalesce. In figure 3 it can be seen that the greatest stress concentration factor is not necessarily associated with the greatest total number of broken filaments. This is especially true in the case of the longer cuts, due to the fact that the stress concentration factors for double cuts increase more rapidly with cut length than do the factors for single cuts across a comparable number of filaments. The results suggest that a design criterion based on the residual strength of a structural component weakened by a single cut of prescribed length can be unconservative, even though only cuts of lesser length are present.

Shear force concentration factor for a single cut.- A result which was not presented in reference 4, but which can be extracted from the analysis is the magnitude of the most severe matrix shear force due to a single cut of arbitrary length. In the case of a single cut the most severe matrix shear force occurs in the neighborhood of each end of the cut. From reference 4, for a cut which starts at the zeroeth filament and severs n filaments, the load and displacement of the i^{th} filament are given by

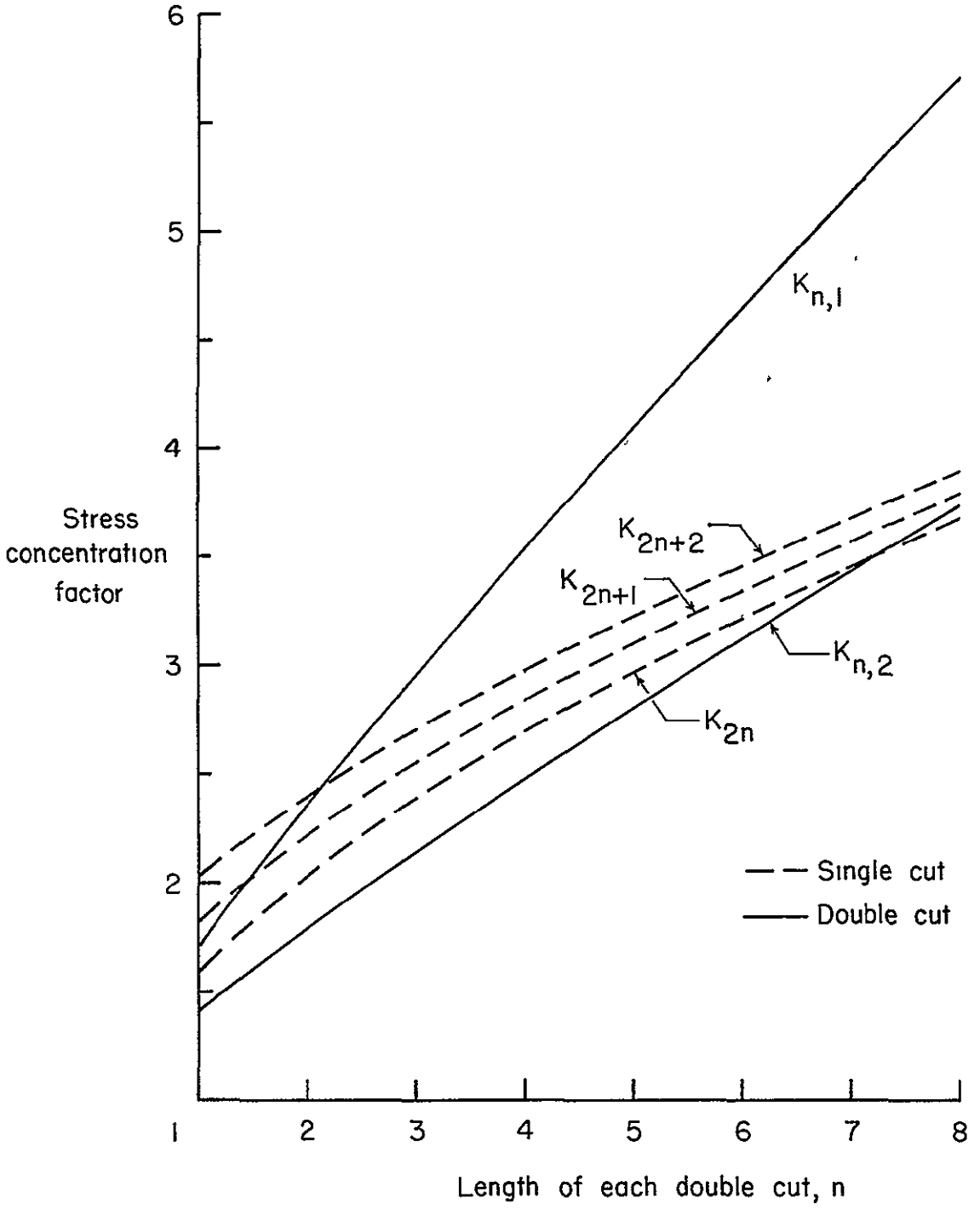

Figure 3. Comparison of filament stress concentration factors for single and double cuts

$$P_i(\xi) = 1 + \sum_{r=0}^{n-1} N_{i-r}(\xi)U_r(0) \tag{22}$$

$$U_i(\xi) = \xi + \sum_{r=0}^{n-1} V_{i-r}(\xi)U_r(0) \tag{23}$$

with

$$0 = 1 + \sum_{r=0}^{n-1} N_{i-r}(0)U_r(0), \quad 0 \leq i \leq n-1 \tag{24}$$

The most severe (nondimensional) shear force is given by $S_{n-1}(0)$ (see equation (23) and the second of equations (10)), which is merely

$$S_{n-1}(0) = -U'_{n-1}(0)$$

since $U_n(0) = 0$ because the n^{th} filament is intact, and $U_{n-1}(0)$ is the nondimensional displacement of the end of the $(n-1)^{th}$ filament. From symmetry considerations this can be written as

$$S_{n-1}(0) = -U_o(0)$$

or

$$S_{max} = \left|U_o(0)\right| \tag{25}$$

where S_{max} is defined as the peak magnitude of the most severe matrix shear force. Of course, $U_o(0)$ varies with the number of broken

filaments and is found by solution of equations (24) for the appropriate value of n.

Solution of equations (24) for the first six values of n yields the following values of S_{max}.

n	$\frac{4}{\pi} S_{max}$
1	1
2	3/2
3	15/8
4	35/16
5	315/128
6	693/256

Inspection of the first six values indicates that they conform to the expression

$$\frac{4}{\pi} S_{max} = \frac{(2n - 1)!}{2^{2n-2}\left[(n - 1)!\right]^2}, \quad n = 1,2,3,\ldots \tag{26}$$

This formula has been shown in Appendix C to hold for all positive values of n. The quantity $\frac{4}{\pi} S_{max}$ is seen to be the ratio of the maximum shear force for $n > 1$ to the maximum shear force for a single broken filament. Hence, it can be viewed as a matrix shear force "concentration factor," in the sense that it describes the growth of the maximum shear force with increasing cut length. In this context, its comparison with the filament stress concentration factor for a single cut (see equation (19)) is appropriate. Therefore, these two quantities have been plotted in figure 4 for values of n

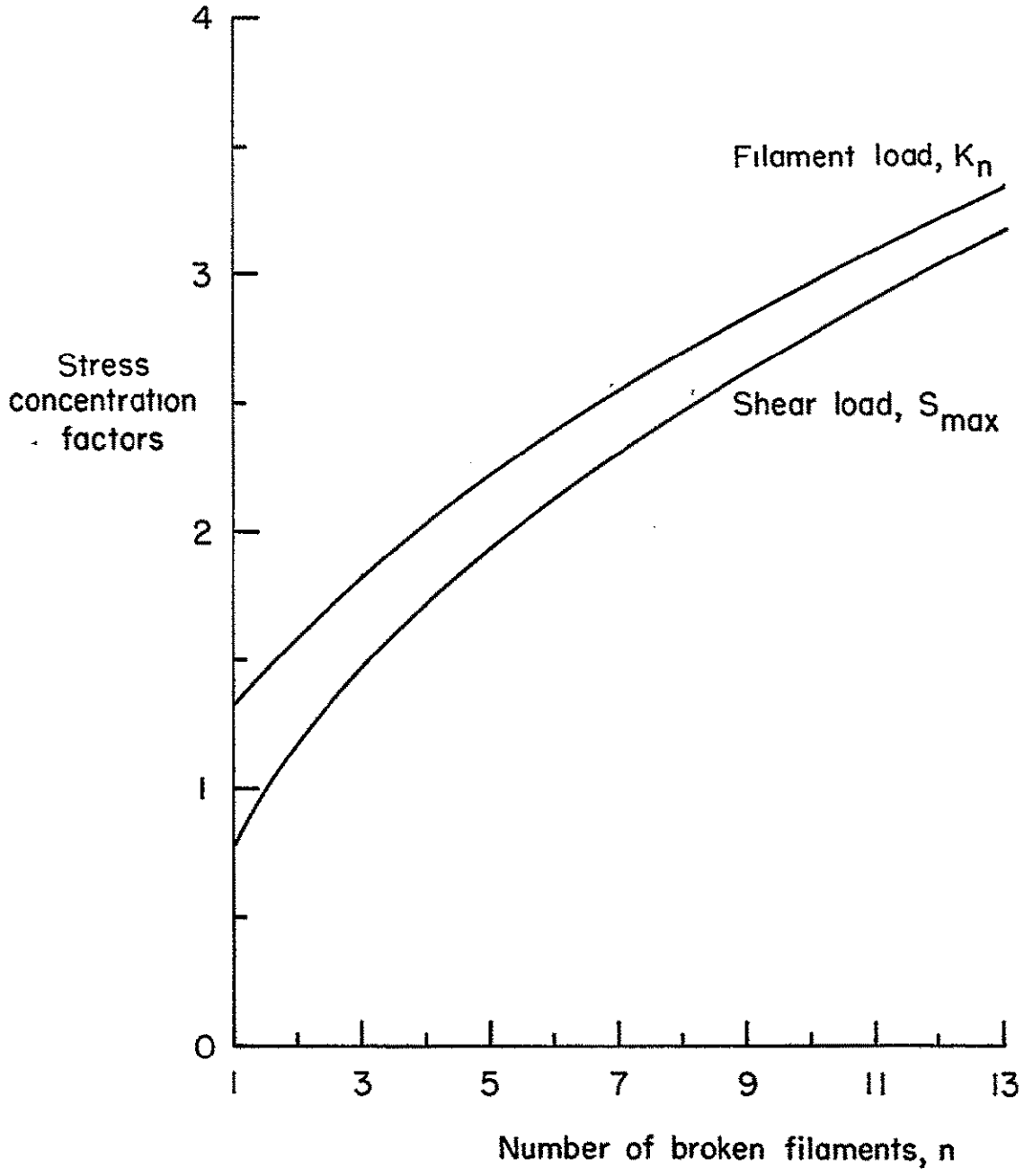

Figure 4. Single-cut concentration factors for filament stress and matrix shear force

up to 13. Both factors are unbounded as n approaches infinity. However, their relative magnitudes for large n can be determined by writing equation (19) in the form

$$K_n = \frac{2^{2n}\, n!(n+1)!}{(2n+1)!}$$

and forming the ratio

$$\frac{\frac{4}{\pi} S_{max}}{K_n} = \frac{n(2n+1)\left[(2n)!\right]^2}{2^{4n-1}(n+1)(n!)^4} \tag{27}$$

By the use of asymptotic formulas for the factorial functions, it is found that

$$\frac{S_{max}}{K_n} \to 1, \text{ as } n \to \infty \tag{28}$$

Equations (27) and (28) indicate that the dimensionless maximum matrix shear force and tensile force in the filaments are of comparable magnitude for all values of n; however, as seen in figure 4, the shear force initially increases more rapidly with cut length than does the filament tensile force. This result suggests that some composites might be more prone to tensile failure when weakened by small flaws, but more susceptible to matrix shear failure when larger flaws are present.

Tensile stress concentration factors for periodic collinear cuts.- The periodic collinear cut configuration is illustrated in figure 5.

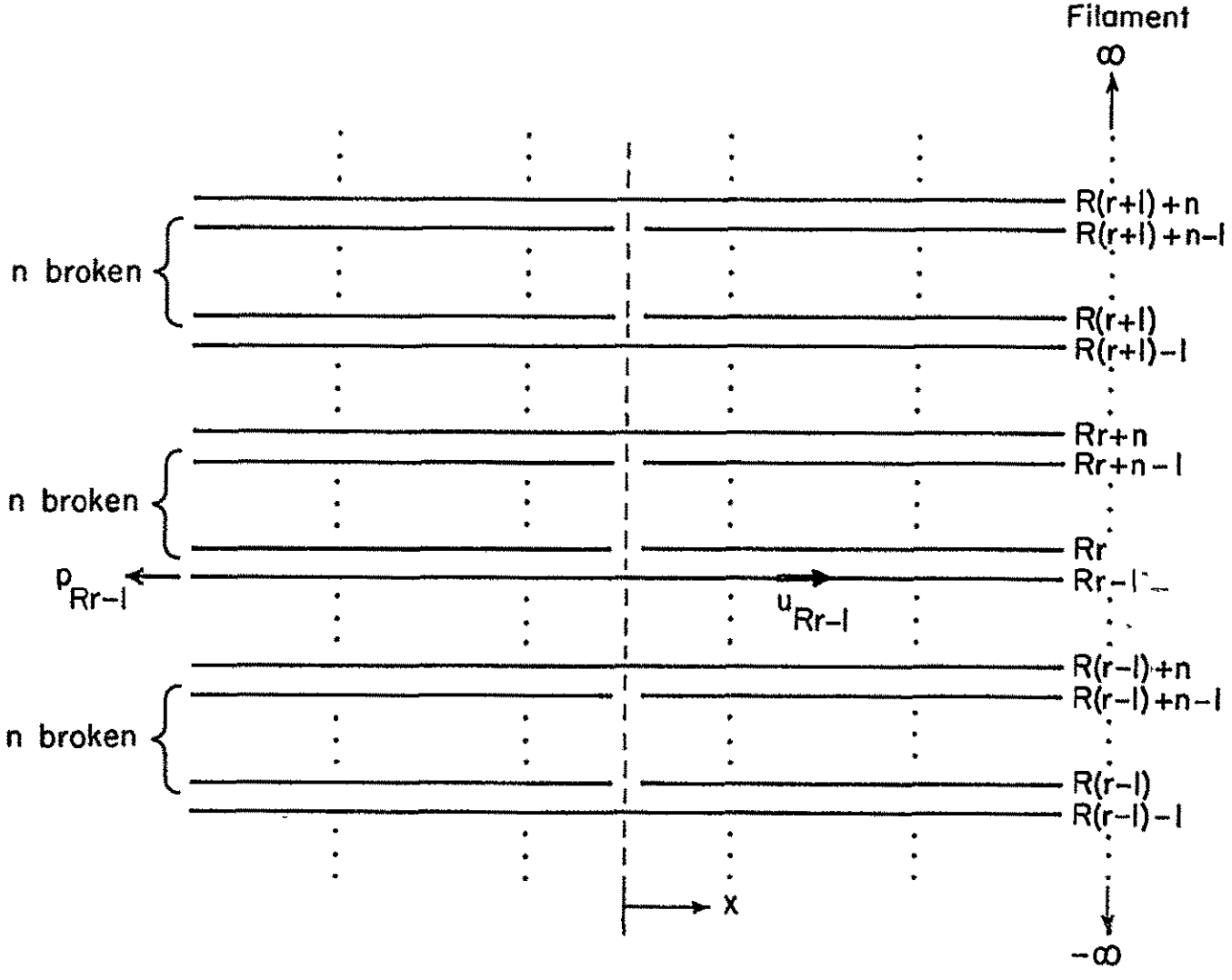

Figure 5. Coordinate and notation systems for periodic collinear cuts

Each cut is across n filaments. The period of the cuts, that is, the distance (in number of filaments) between the first broken filaments in succeeding cuts, is denoted by the integer R. The periodic configuration is of interest because, within the limitations of the present model, the periodic-cut problem is equivalent to the problem of a central transverse cut across n filaments in a filamentary strip which is R filaments wide. Of course, for the problem to be meaningful, R must be greater than n. The expressions for load and displacement are given by equations (11) subject to the mixed boundary conditions

$$P_i(0) = 0, \quad i = Rr, Rr + 1, \ldots, Rr + n - 1, \quad r = 0, \pm 1, \pm 2, \ldots \tag{29}$$

and

$$U_i(0) = 0 \quad \text{for all other } i$$

where, for convenience, one of the cuts is begun at the zeroeth filament. Application of boundary conditions (29) to equations (11) yields

$$P_i(\xi) = 1 + \sum_{m=-\infty}^{\infty} \Big\{ N_{i-Rm}(\xi) U_{Rm}(0) + N_{i-Rm-1}(\xi) U_{Rm+1}(0) + \ldots + N_{i-Rm-n+1}(\xi) U_{Rm+n-1}(0) \Big\} \tag{30}$$

$$U_i(\xi) = \xi + \sum_{m=-\infty}^{\infty} \Big\{ V_{i-Rm}(\xi)U_{Rm}(0) + V_{i-Rm-1}(\xi)U_{Rm+1}(0) + \dots + V_{i-Rm-n+1}(\xi)U_{Rm+n-1}(0) \Big\} \tag{31}$$

since $U_i(0) = 0$ for other values of i, and

$$0 = 1 + \sum_{n=-\infty}^{\infty} \Big\{ N_{i-Rm}(0)U_{Rm}(0) + N_{1-Rm-1}(0)U_{Rm+1}(0) + \dots + N_{i-Rm-n+1}(0)U_{Rm+n-1}(0) \Big\}, \quad Rr \leq i \leq Rr + n - 1, \quad r = 0, \pm 1, \pm 2, \dots \tag{32}$$

which expresses the condition of zero load on the ends of the broken filaments. Replacing i by $Rr + j$ in equations (32) yields

$$0 = 1 + \sum_{m=-\infty}^{\infty} \Big\{ N_{R(r-m)+j}(0)U_{Rm}(0) + N_{R(r-m)+j-1}(0)U_{Rm+1}(0) + \dots + N_{R(r-m)+j-n+1}(0)U_{Rm+n-1}(0) \Big\}, \quad 0 \leq j \leq n - 1$$

Now letting $k = r - m$ gives

$$0 = 1 + \sum_{k=-\infty}^{\infty} \Big\{ N_{Rk+j}(0)U_{R(r-k)}(0) + N_{Rk+j-1}(0)U_{R(r-k)+1}(0) + \dots + N_{Rk+j-n+1}(0)U_{R(r-k)+n-1}(0) \Big\}, \quad 0 \leq j \leq n - 1 \tag{33}$$

However, due to the periodicity of the displacements, $U_{R(r-k)}(0) = U_o(0)$, $U_{R(r-k)+1} = U_1(0)$, etc., so that equations (33) become

$$0 = 1 + \sum_{k=-\infty}^{\infty} \Big\{ N_{Rk+j}(0)U_o(0) + N_{Rk+j-1}(0)U_1(0) + \dots + N_{Rk+j-n+1}(0)U_{n-1}(0) \Big\}, \quad 0 \leqq j \leqq n-1$$

which can also be written as

$$0 = 1 + U_o(0) \sum_{k=-\infty}^{\infty} N_{Rk+j}(0) + U_1(0) \sum_{k=-\infty}^{\infty} N_{Rk+j-1}(0) + \dots + U_{n-1}(0) \sum_{k=-\infty}^{\infty} N_{Rk+j-n+1}(0), \quad 0 \leqq j \leqq n-1 \tag{34}$$

which are merely n linear algebraic equations for the $U_j(0)$'s. It remains to evaluate the coefficients given by the infinite series. This has been done in Appendix D, and the results are

$$\sum_{k=-\infty}^{\infty} N_{Rk+j}(0) = \frac{1}{R} \left\{ \cot \frac{\pi}{R}\left(j - \frac{1}{2}\right) - \cot \frac{\pi}{R}\left(j + \frac{1}{2}\right) \right\} \tag{35}$$

A further slight simplification of equations (30), (31), and (34) is afforded by noting the symmetry of the displacements in each cut, which gives $U_o(0) = U_{n-1}(0)$, $U_1(0) = U_{n-2}(0)$, etc. This simplification

reduces the order of the system by roughly half (actually, by $n/2$ equations for n even, and by $\frac{n-1}{2}$ for n odd).

The filament stress concentration factor is obtained by calculating the maximum load in the first intact filament at either end of any of the cuts. For this purpose, the n^{th} filament is chosen; thus the stress concentration factor is given by

n even.

$$K_n^R = P_n(0) = 1 + U_o(0) \sum_{k=-\infty}^{\infty} \left\{ N_{n-Rk}(0) + N_{1-Rk}(0) \right\}$$

$$+ U_1(0) \sum_{k=-\infty}^{\infty} \left\{ N_{n-Rk-1}(0) + N_{2-Rk}(0) \right\} + \cdots$$

$$+ U_{n/2\ -1}(0) \sum_{k=-\infty} \left\{ N_{n/2\ -Rk+1}(0) + N_{n/2\ -Rk}(0) \right\} \tag{36}$$

n odd:

$$K_n = 1 + U_o(0) \sum_{k=-\infty}^{\infty} \left\{ N_{n-Rk}(0) + N_{1-Rk}(0) \right\}$$

$$+ \cdots + U_{\frac{n-3}{2}}(0) \sum_{k=-\infty}^{\infty} \left\{ N_{\frac{n+3}{2} - Rk}(0) + N_{\frac{n-1}{2} - Rk}(0) \right\}$$

$$+ U_{\frac{n-1}{2}}(0) \sum_{k=-\infty}^{\infty} N_{\frac{n+1}{2} - Rk}(0)$$

where it should be noted that $N_{i-Rk}(0) = N_{Rk-i}(0)$, and where the $U_1(0)$'s have been calculated from equations (34) for specified values of n and R (cut length and period).

The stress concentration factor K_n^R has been calculated for values of n from 1 to 6, and for values of R up to 36. The results are presented in Table 2. The results are plotted in figure 6, for a limited range of R - n, in terms of net section load (average load in the unbroken filaments) rather than average load at infinity, in keeping with customary engineering practice. Again, although the results are meaningful only for integral values of R - n, they are plotted as continuous curves for ease of illustration. Also plotted in figure 6 are results of an approximate analysis by Dixon (see reference 3), which were employed by Zender and Deaton in reference 9 to convert the infinite-sheet results of Hedgepeth (reference 4) to a form usable for analyzing their experimental data on strips of filamentary material. As can be seen in figure 6, the results of the approximate analysis of Dixon are in close agreement with the present results except for cuts whose length approaches the width of the strip. In this range, the predictions of reference 3 are seen to underestimate the stress concentration factor. However, in the range of cut length to strip width ratios of practical interest, Dixon's approximate formula, although slightly unconservative, is quite sufficiently accurate to justify its use. For example, although the comparison is not shown here, Dixon's results, when applied to the data of Zender

Table 2. Filament stress concentration factors for periodic collinear cuts (based on net section load)

Net section, R-n	Cut length, n					
	1	2	3	4	5	6
1	1.000	1.000	1.000	1.000	1.000	1.000
2	1.000	1.000	1.000	1.000	1.000	1.000
3	1.061	1.085	1.098	1.105	1.110	1.113
4	1.106	1.155	1.182	1.199	1.210	1.218
5	1.138	1.209	1.250	1.277	1.295	1.308
6	1.163	1.251	1.305	1.342	1.367	1.386
7	1.182	1.285	1.351	1.396	1.429	1.453
8	1.198	1.314	1 390	1.443	1.482	1.512
9	1.210	1.337	1.422	1.483	1.529	1.563
10	1.221	1.357	1.451	1.518	1.569	1.609
11	1.229	1.374	1.475	1.549	1.606	1.650
12	1.237	1.389	1.497	1.576	1.638	1.687
15	1.254	1.424	1.548	1.642	1.717	1.778
20	1.272	1.462	1.605	1.718	1.810	1.886
25	1.284	1.487	1.643	1.769	1.873	1.961
30	1.291	1.504	1.670	1.806	1.919	2.016

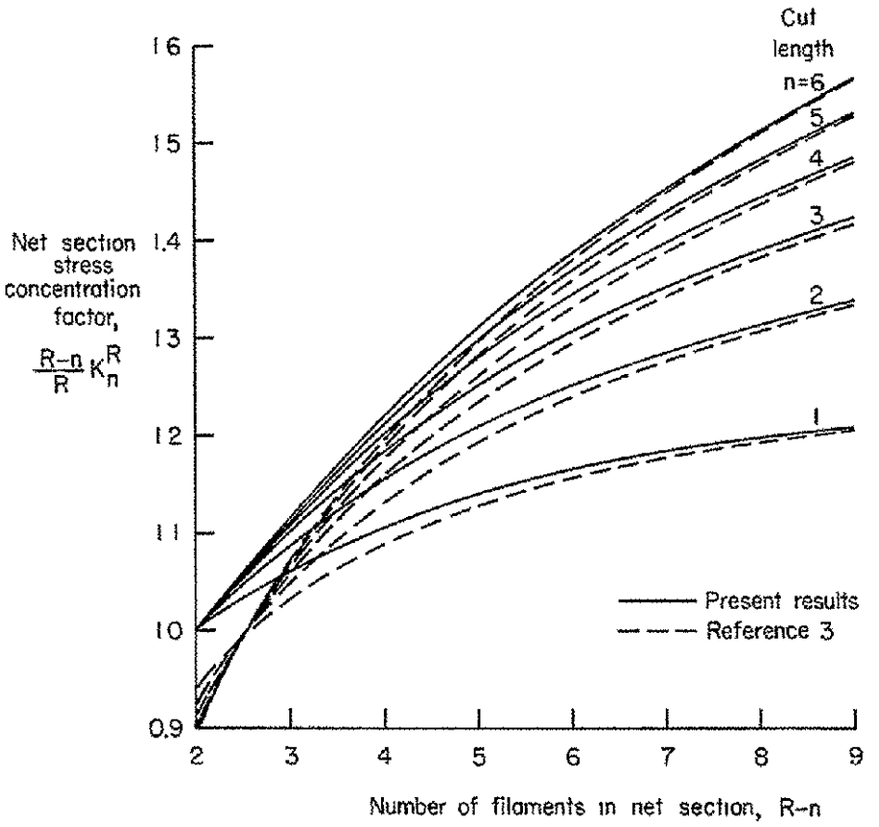

Figure 6. Filament stress concentration factors for periodic collinear cuts

and Deaton (reference 9), were found to be indistinguishable from the present results.

Dynamic stress concentration factors for two collinear cuts.- In reference 4, dynamic stress concentration factors were found for cases in which a cut is suddenly introduced in a stretched filament sheet and, in a separate analysis, an apparent upper limit of 1.27 was found for the dynamic response factor (ratio of maximum dynamic to static stress concentration factor). Investigated were cuts across one, two, and three filaments, and the limiting case of a finite-length slit in a so-called continuous stringer sheet which is an orthotropic medium with finite extensional stiffness in the longitudinal direction, infinite extensional stiffness in the transverse direction, and finite shear stiffness.

In order to investigate the possibility of a departure from the trend for a single cut, the analysis of reference 4 has been extended to two of the simplest double-cut cases. In each case the two cuts are separated by a single intact filament, with totals of two and four filaments being broken in the two cases. The dynamic results have been obtained by extending the single-cut dynamic analysis of reference 4 in the same way that the static analysis is extended. The Laplace transform is applied to equations (7) and (8), and initial conditions (9) are employed to obtain an expression for the transformed stress concentration factor. Then a term-by-term inversion of the transformed stress concentration factor is carried out to obtain a series expression for the dynamic stress concentration factor which can be made as accurate

as desired by the retention of a sufficient number of terms. The dynamic analysis is presented in Appendix E. The reader is referred to reference 4 for a complete discussion of the analytical technique.

The results are plotted in figure 7, where some of the results from reference 4 are reproduced for purposes of comparison. By comparison of the peak dynamic double-cut values with the appropriate static values from Table 1, it is found that the dynamic response factors for the cases of two and four broken filaments are 1.22 and 1.23, respectively. This result is in keeping with the trend noted in reference 4 for single cuts. The fact that additional double-cut calculations have not been made because of their rapidly increasing complexity precludes the drawing of sweeping conclusions concerning the overall behavior of the double-cut dynamic response factor, nevertheless, radical departure from the single-cut trend appears to be unlikely. At the least, the present results do nothing to contradict the conclusion reached in reference 4 that dynamic effects appear to be of secondary importance in composite materials of the type investigated.

Filament and Matrix Loads

In this section, expressions are obtained for the most severe matrix shear forces for some single-cut and double-cut cases, in order to illustrate their behavior in the neighborhood of the cuts, and how they vary along the filaments. In addition, loads in broken filaments are calculated for some single-cut cases, and with the aid of an idealized model their load-recovery characteristics are examined in

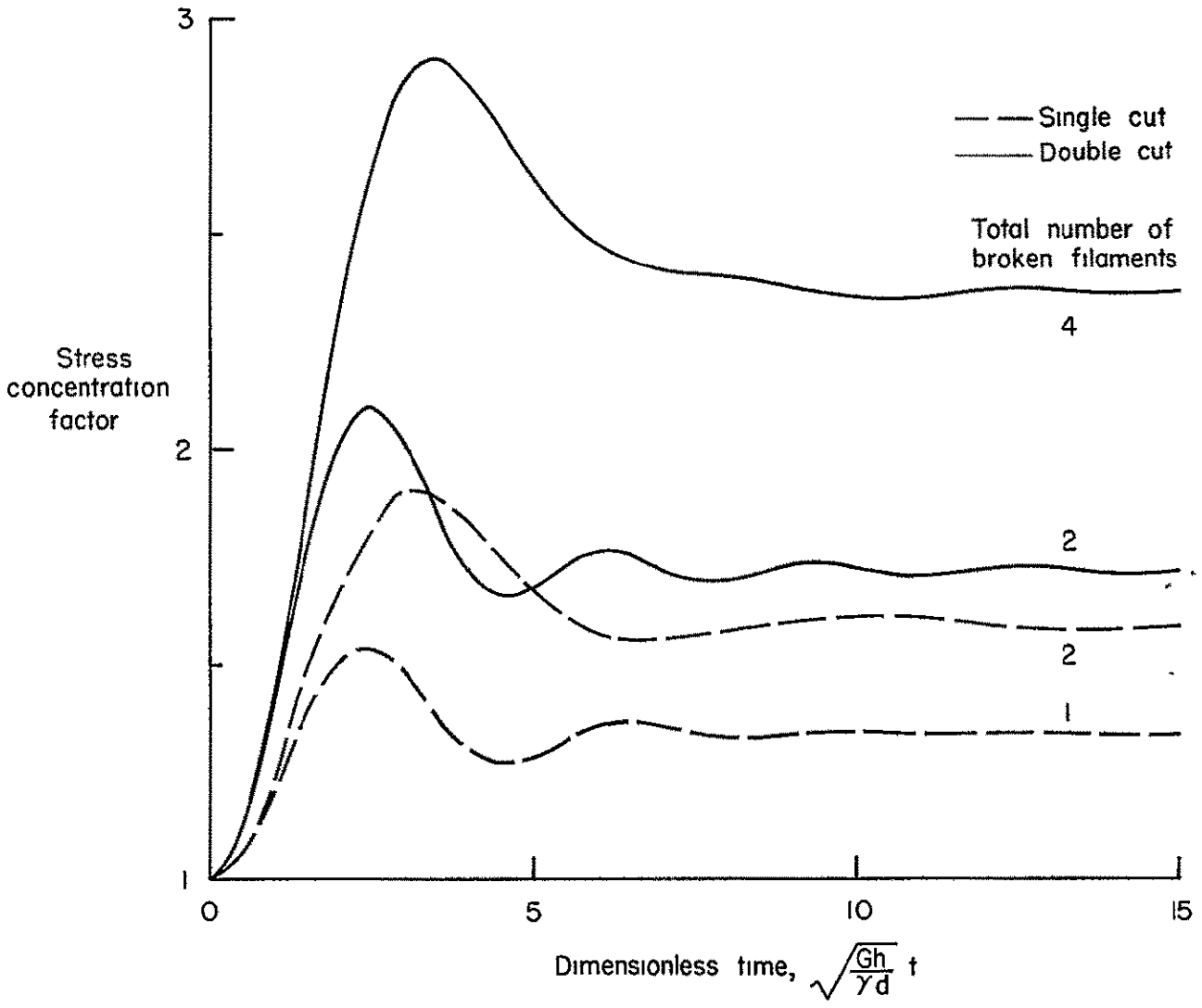

Figure 7. Dynamic stress concentration factors

connection with a current composite tensile failure model (see reference 8).

Matrix shear loads.- The dimensionless shear force per unit length between the n^{th} and $(n+1)^{th}$ filaments is given by

$$S_n(\xi) = U_{n+1}(\xi) - U_n(\xi) \tag{37}$$

In either a single-cut or double-cut configuration, the greatest matrix shear load is between a broken filament and an unbroken one. In the case of a double cut, the unbroken filament is an interior one. To find the matrix shear forces in a single-cut problem, the solutions to equations (24) for a specified number of broken filaments are substituted into equation (23), yielding the displacements of the filaments. Then the appropriate displacements are substituted into equation (37) to obtain the matrix shear load as a function of the longitudinal distance from the cut. For a double cut either equations (A4) or (A10) are solved, depending on the number of interior filaments, and their solutions are substituted into the second of equations (A3) or (A9), respectively, to obtain displacements which, in turn, are substituted into equation (37) to obtain the matrix shear load of interest. The influence functions $V_n(\xi)$ required in equations (23), (A3), or (A9) are given by equation (16).

The results for single cuts across one, two, and three filaments are:

Single cut across one filament:

$$S_0(\xi) = \frac{\pi}{4}\left[\frac{2}{\pi\xi} + 2\left\{L_0(2\xi) - I_0(2\xi)\right\} - \frac{1}{\xi}\left\{L_{-1}(2\xi) - I_1(2\xi)\right\}\right] \tag{38}$$

where $S_0(0) = -\frac{\pi}{4}$.

Single cut across two filaments:

$$S_1(\xi) = \frac{3\pi}{8}\left[\frac{6}{\xi^2}\left\{I_0(2\xi) - L_0(2\xi)\right\} + \frac{2}{\xi}\left(2 + \frac{3}{\xi^2}\right)\left\{L_{-1}(2\xi) - I_1(2\xi)\right\} - \frac{12}{\pi\xi^3}\right] \tag{39}$$

where $S_1(0) = -\frac{3\pi}{8}$.

Single cut across three filaments:

$$S_2(\xi) = -\frac{3\pi}{16}\left[\left(4 + \frac{87}{\xi^2} + \frac{300}{\xi^4}\right)\left\{I_0(2\xi) - L_0(2\xi)\right\} + \frac{1}{\xi}\left(20 + \frac{237}{\xi^2} + \frac{300}{\xi^4}\right)\left\{L_{-1}(2\xi) - I_1(2\xi)\right\} - \frac{4}{\pi\xi} - \frac{74}{\pi\xi^3} - \frac{600}{\pi\xi^5}\right], \tag{40}$$

where $S_2(0) = -\frac{15}{32}\pi$.

The results for double cuts are:

Two cuts, each across one filament, with one interior filament:

$$\bar{S}_0(\xi) = \frac{15\pi}{56}\left[2\left(2 + \frac{3}{\xi^2}\right)\left\{I_0(2\xi) - L_0(2\xi)\right\} + \frac{6}{\xi}\left(1 + \frac{1}{\xi^2}\right)\left\{L_{-1}(2\xi) - I_1(2\xi)\right\} - \frac{4}{\pi\xi} - \frac{12}{\pi\xi^3}\right], \tag{41}$$

where $\bar{S}_0(0) = \frac{15}{56}\pi$.

Two cuts, each across two filaments, with one interior filament:

$$\bar{S}_o(\xi) = \frac{5565\pi}{2(6512)}\left[2\left(2 + \frac{3}{\xi^2}\right)\left\{I_o(2\xi) - L_o(2\xi)\right\} + \frac{6}{\xi}\left(1 + \frac{1}{\xi^2}\right)\left\{L_{-1}(2\xi) - I_1(2\xi)\right\}\right.$$

$$- \frac{4}{\pi\xi} - \frac{12}{\pi\xi^3} - \frac{51}{53}\left(4\left(1 + \frac{12}{\xi^2} + \frac{30}{\xi^4}\right)\left\{I_o(2\xi) - L_o(2\xi)\right\} + \frac{6}{\xi}\left(3 + \frac{18}{\xi^2}\right.\right.$$

$$\left.\left. + \frac{20}{\xi^4}\right)\left\{L_{-1}(2\xi) - I_1(2\xi)\right\} - \frac{4}{\pi\xi} - \frac{56}{\pi\xi^3} - \frac{240}{\pi\xi^5}\right)\Bigg] \qquad (42)$$

where $\bar{S}_o(0) = \frac{5565}{2(6512)}\pi$, and the bars are used to denote double-cut shear loads. A comparison of equations (41) and (42) will indicate how rapidly the complexity of double-cut shear force calculations increases with cut length.

These most severe shear loads are plotted in normalized form in figure 8 Also shown in figure 8 for easy reference is a table of their maximum amplitudes. As can be seen, the normalized shear loads are distinguished from one another mainly by their rates of decay with distance along the filaments, the decay being more gradual for longer cuts. It might also be noted that the peak shear loads for double cuts are less severe than those for single cuts across comparable or even smaller numbers of filaments. This would appear to be due to the fact that double cuts are directly adjacent to larger numbers of intact filaments (three or four) than are single cuts (always two); hence, the load lost by the broken filaments is distributed over a larger number of intact filaments in the case of double cuts.

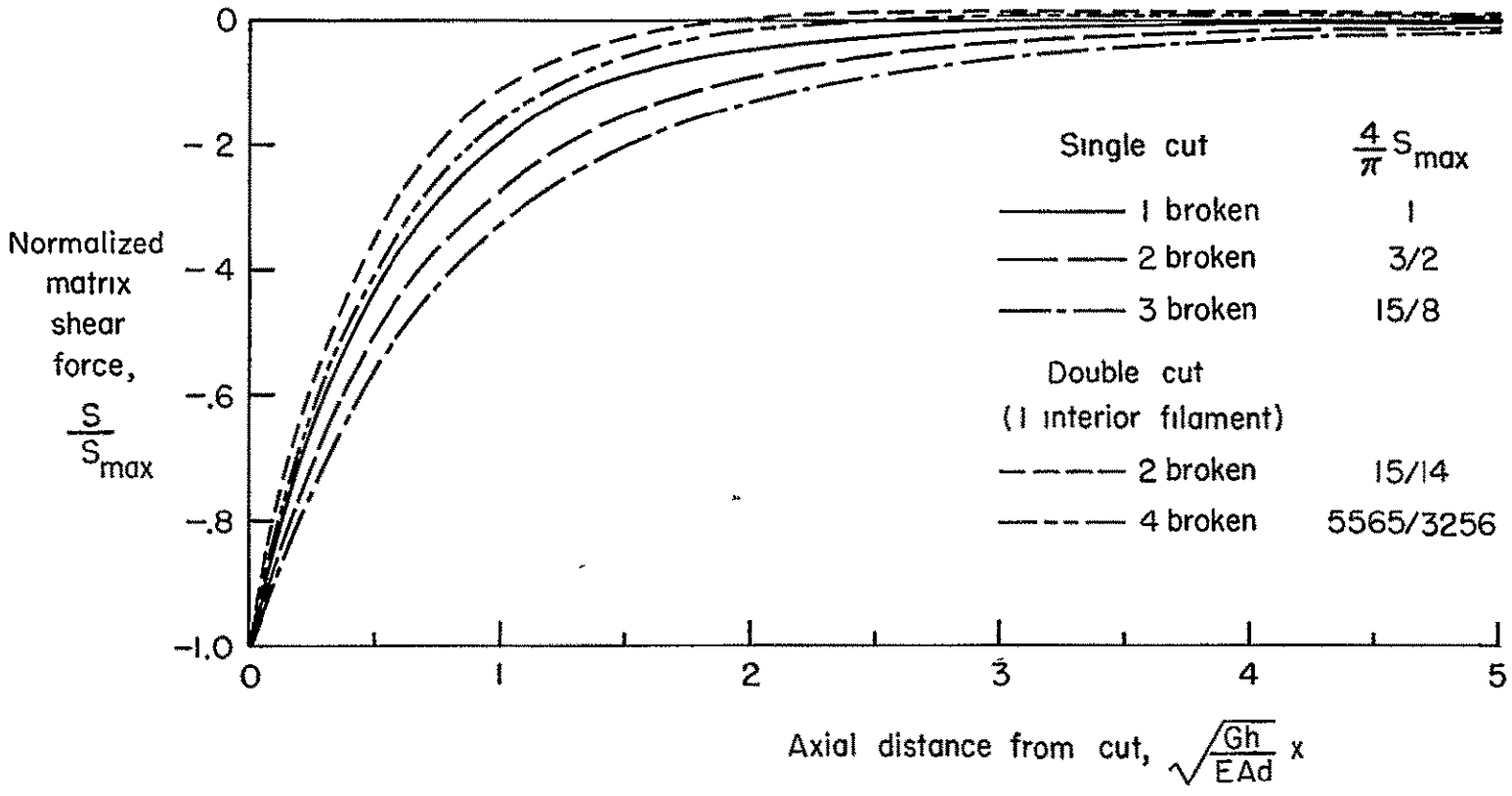

Figure 8. Variation of most severe matrix shear forces with axial distance from the cut

Loads in broken filaments.- The calculation of loads in broken filaments is of interest because it facilitates an examination of the ability of the composite matrix to transfer the load back into the broken filaments and, hence, gives a measure of the degree of localization of the perturbed stress state.

For a single cut across n consecutive filaments (starting with the zeroeth filament), the load in the i^{th} filament is given by

$$P_i(\xi) = 1 + \sum_{m=0}^{n-1} N_{i-m}(\xi)U_m(0)$$

where the broken filaments are identified by $i = 0,1, \ldots, n - 1$. Each $U_m(0)$ is one of a unique set associated with a specific value of n. The influence function $N_j(\xi)$ is given by equation (17). Loads in the broken filaments have been calculated for a single cut across one, two and three filaments. The results are:

One broken filament:

$$P_o(\xi) = 1 - \frac{\pi}{2}\left\{L_{-1}(2\xi) - I_1(2\xi)\right\} \tag{43}$$

where $P_o(0) = 0$.

Two broken filaments:

$$P_o(\xi) = P_1(\xi) = 1 - \frac{3\pi}{4}\left[\frac{1}{\xi}\left\{L_o(2\xi) - I_o(2\xi)\right\} - \frac{1}{\xi^2}\left\{L_{-1}(2\xi) - I_1(2\xi)\right\} + \frac{2}{\pi\xi^2}\right] \tag{44}$$

where $P_o(0) = P_1(0) = 0$.

Three broken filaments:

$$P_o(\xi) = P_2(\xi) = 1 - \frac{3\pi}{8}\left[\left(2 + \frac{22}{\xi^2} + \frac{30}{\xi^4}\right)\left\{L_{-1}(2\xi) - I_1(2\xi)\right\}\right.$$
$$\left. - \frac{1}{\xi}\left(7 + \frac{30}{\xi^2}\right)\left\{L_o(2\xi) - I_o(2\xi)\right\} - \frac{4}{\pi\xi^2} - \frac{60}{\pi\xi^4}\right] \qquad (45)$$

$$P_1(\xi) = 1 - \frac{3\pi}{8}\left[\left(2 + \frac{5}{\xi^2}\right)\left\{I_1(2\xi) - L_{-1}(2\xi)\right\}\right.$$
$$\left. + \frac{5}{\xi}\left\{L_o(2\xi) - I_o(2\xi)\right\} + \frac{10}{\pi\xi^2}\right] \qquad (46)$$

where $P_o(0) = P_1(0) = P_2(0) = 0$.

The results are plotted in figure 9. The 90 percent load-recovery level is noted on figure 9 for later reference. It can be seen that the longitudinal distance required by a broken filament to recover a given fraction of its far-field load increases considerably with cut length. This result is of interest in connection with the statistical failure analysis of reference 8, in which a significant parameter is the so-called "ineffective length" of a broken filament. The ineffective length is defined there as that portion of the length of a broken filament over which it supports less than 90 percent of its share of the load. In the next section, an idealized model is employed for calculating ineffective lengths with the aid of figure 9, and the implications of the results for the statistical failure analysis of reference 8 are briefly discussed.

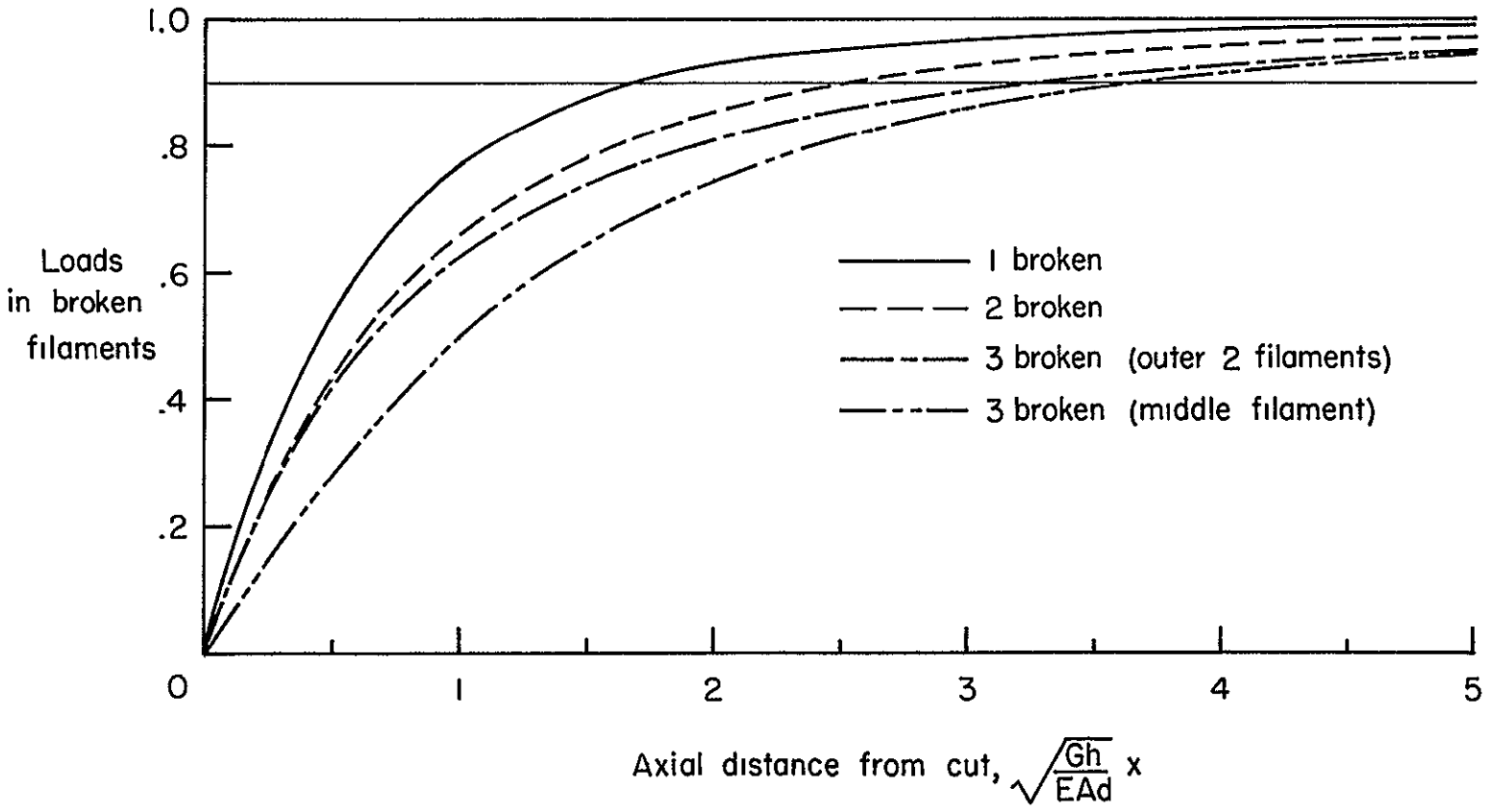

Figure 9. Loads in broken filaments near a single cut

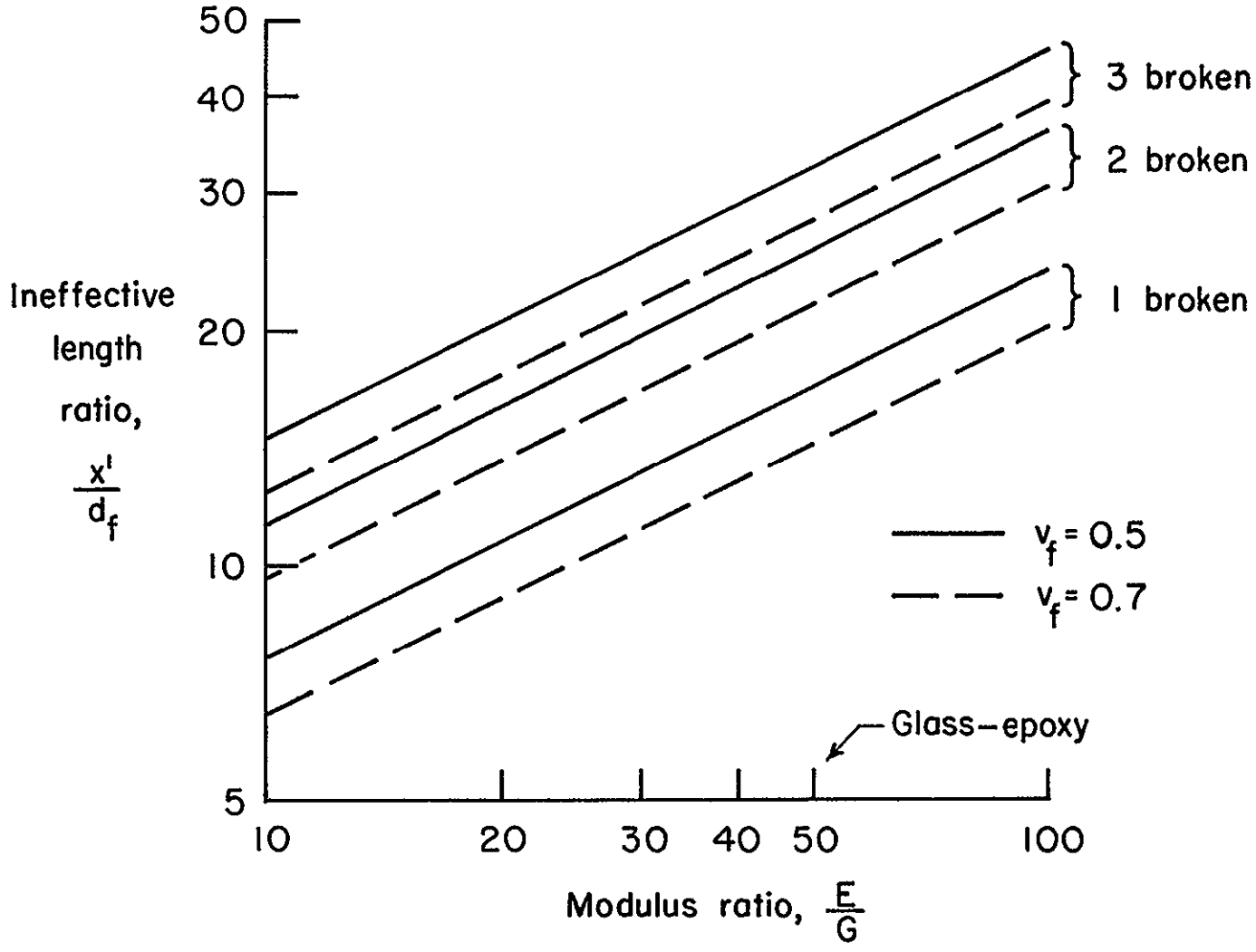

Figure 10. Variation of ineffective filament length near a single cut

Ineffective length calculation.- Studies cited in references 6 and 8 suggest that the ineffective length, based on a load-recovery fraction of 90 percent of a single broken filament embedded in a matrix, can vary from one up to several hundred filament diameters, depending on the geometry of the composite and the mechanical properties of its constituents. Calculations have been made in reference 8, for example, of ineffective length as a function of filament volume fraction (ratio of filament volume to composite volume), v_f, and E/G, the ratio of filament Young's modulus to matrix shear modulus. The results are presented in the form of a family of curves, each member of which corresponds to a particular volume fraction.

In the case of a composite containing a cut, an additional parameter which would be expected to influence the ineffective length is the number of broken filaments. With the aid of an idealized model, the present results can be used to obtain an indication of the influence of this parameter. A typical cross section of this model is shown in the sketch. For the present calculations, it is assumed that the thickness of the sheet is equal to the filament diameter. Then for this model the filament volume fraction is given by $v_f = \frac{\pi d_f}{4d}$, where d_f is the filament diameter and d is the filament spacing.

In terms of the pertinent mechanical and geometrical parameters, the axial distance from the cut is given by

$$x = \sqrt{\frac{EAd}{Gh}}\,\xi$$

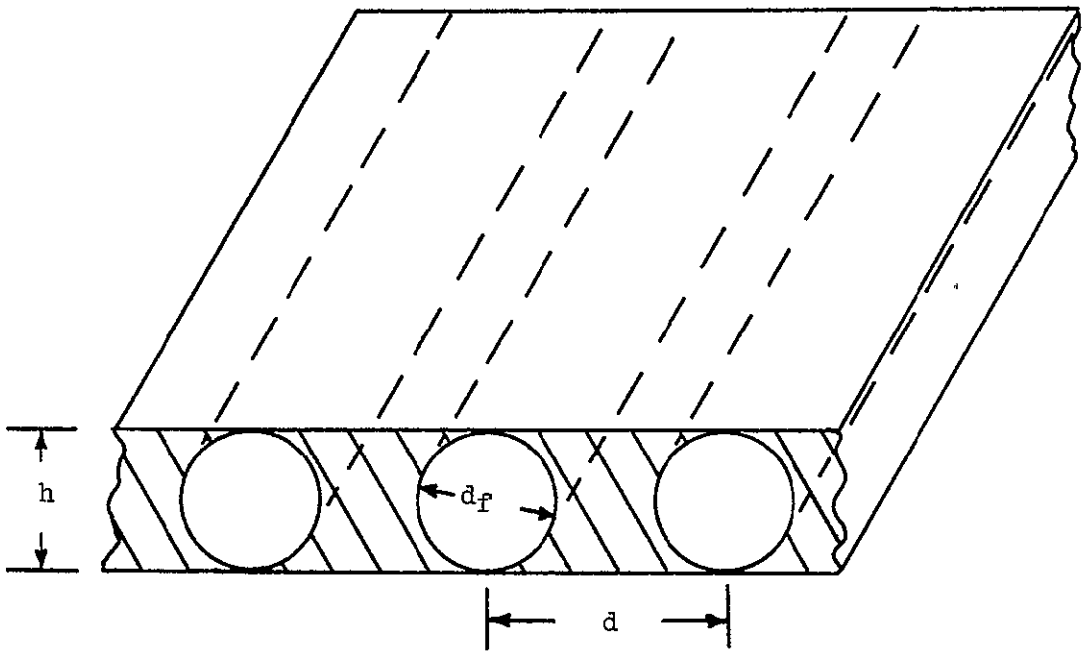

which for the idealized model becomes

$$\frac{x}{d_f} = \frac{\pi}{4}\sqrt{\frac{E}{Gv_f}}\,\xi \tag{47}$$

In order to obtain estimates of ineffective length changes due to the breaking of additional filaments, it is necessary to determine the values of ξ, denoted by ξ', at which the broken filaments of interest have recovered 90 percent of their far-field load. These values of ξ, along with the appropriate values of E/G and v_f, are then substituted into equation (47) to obtain values of the nondimensional ineffective length, denoted by $\frac{x'}{d_f}$.

This procedure has been carried out for two values of v_f and a range of values of E/G. The cases of cuts across one, two and three filaments have been considered In the case of a cut across three filaments, the 90 percent recovery figure applies to either of the outer filaments in the cut rather than the middle filament, which would have yielded even greater values of ineffective length. The results are presented in figure 10

The mathematical model employed in reference 8 consists of a single filament encased in a thin layer of shear-carrying material (binder) which, in turn, is embedded in an infinite body to which are assigned the average stiffness properties of the composite material. Hence, interaction between neighboring filaments is ignored. In addition, shear stresses in the average material are assumed to decay in a negligible distance from its interface with the thin layer of binder material. Because of these basic differences, the results of reference 8 are not included in figure 10.

It should be noted, however, that the results of reference 8 yield a single curve for each filament volume fraction, whereas the present results yield a family of curves, each member of which corresponds to a different number of broken filaments. As can be seen, large changes in ineffective filament length can result from varying the number of broken filaments The failure analysis of reference 8, however, depends on a fixed value of ineffective length, regardless of the number and distribution of breaks in the composites. The present results suggest

that changes in ineffective length due to flaw size should be accounted for in statistical studies of the ultimate strength of filamentary composites. It might also be noted that the present results predict a more gradual recovery of load by broken filaments than does the analysis of reference 8.

CONCLUDING REMARKS

Analyses have been conducted of the loads and deformations in a filament-stiffened sheet weakened by two collinear cuts and by periodic collinear cuts. Also, some results have been obtained for the case of a single cut in addition to those previously reported. It has been found that significant interaction between collinear cuts is largely restricted to cases in which the distance between cuts is no greater than the cut length. It is seen that two closely spaced cuts can cause greater stress concentration than a single cut across a comparable total number of filaments. In the case of periodic collinear cuts, exact results indicate that a stress concentration factor derived for a transverse cut in an elastic strip in an earlier approximate analysis by Dixon (reference 3) is adequate for practical applications, although it is somewhat unconservative for cut lengths which approach the strip width.

Limited calculations of dynamic stress concentration factors for suddenly introduced collinear cuts support the earlier conclusion that dynamic effects are not of great importance in filamentary composites of the type investigated.

Maximum shear force calculations for single cuts of various lengths, which show that maximum shear forces grow more rapidly with cut length than maximum tensile forces, might be useful in determining whether a damaged composite material is more susceptible to shear failure or tensile failure.

Calculations of loads in broken filaments show significant changes in ineffective filament length with cut length, indicating that statistical strength analyses of composite materials should consider the incorporation of a flaw-size parameter.

The present analyses are based on linear, small-deflection theory of a single filamentary sheet, whereas filamentary composites usually are many filaments thick, and are subject to various nonlinear effects, such as plastic deformations, large deflections and straightening of the filaments. Therefore, it appears that future analytical studies might be fruitfully directed toward analysis of better models of composite materials.

LIST OF REFERENCES

1. Abramowitz, Milton, and Stegun, Irene, editors. 1964. Handbook of Mathematical Functions. National Bureau of Standards AMS no. 55.

2. Carrier, G. F., Krook, M., and Pearson, C. E. 1966. Functions of a Complex Variable, McGraw-Hill Book Co., p. 97.

3. Dixon, J. R. 1960. Stress Distribution Around a Central Crack in a Plate Loaded in Tension, J. Royal Aeronautical Society 64, no. 591.

4. Hedgepeth, John M. 1961. Stress Concentration in Filamentary Structures. NASA TN D-882.

5. Hedgepeth, John M., and Van Dyke, Peter. 1967. Local Stress Concentration in Imperfect Filamentary Composite Materials, J. Composite Materials 1, no. 3, pp. 294-309.

6. Kelly, A., and Davies, G. J. 1965. The principles of the Fiber Reinforcement of Metals, Metallurgical Reviews 10, no. 37.

7. Riordan, John. 1968. Combinatorial Identities, John Wiley and Sons.

8 Rosen, B. Walter. 1965. Mechanics of Composite Strengthening, Fiber Composite Materials, American Society for Metals, pp. 37-75.

9. Zender, George W., and Deaton, Jerry W. 1963 Strength of Filamentary Sheets With One or More Fibers Broken, NASA TN D-1609.

APPENDIX A

EVALUATION OF INFLUENCE FUNCTION $V_n(\xi)$

The influence function $V_n(\xi)$ is given by

$$V_n(\xi) = \frac{1}{\pi}\int_0^{\pi} \cos n\theta \, e^{-2\xi \sin \theta/2} \, d\theta \tag{A1}$$

which can be changed to

$$V_n(\xi) = \frac{1}{\pi}\int_0^{\pi} \cos 2n\theta \, e^{-2\xi \sin \theta} \, d\theta \tag{A2}$$

Let $\xi = e^{-i\pi/2}\,\Phi$; then (A2) becomes

$$V_n = \frac{1}{2\pi}\int_0^{\pi} (e^{2in\theta} + e^{-2in\theta}) e^{2i\Phi \sin \theta} \, d\theta$$

or

$$V_n = \frac{1}{2\pi}\int_0^{\pi} \left[\cos(2\Phi \sin\theta + 2n\theta) + \cos(2\Phi \sin\theta - 2n\theta) \, d\theta\right]$$

$$+ \frac{1}{2\pi}\int_0^{\pi} \left[\sin(2\Phi \sin\theta + 2n\theta) + \sin(2\Phi \sin\theta - 2n\theta) \, d\theta\right]$$

which becomes

$$V_n = \frac{1}{2}\left\{J_{-2n}(2\Phi) + J_{2n}(2\Phi)\right\} + \frac{i}{2\pi}\int_0^{\pi}\left[\sin(2n\theta + 2\Phi \sin\theta) - \sin(2n\theta - 2\Phi \sin\theta)\right]d\theta \quad (A3)$$

where J_{2n} is the Bessel function of the first kind. The remaining integral may be evaluated to give

$$V_n = \frac{1}{2}\left\{J_{-2n}(2\Phi) + J_{2n}(2\Phi)\right\} + \frac{1}{2}\left\{E_{2n}(-2\Phi) - E_{2n}(2\Phi)\right\} \quad (A4)$$

where E_{2n} is the Weber function (see reference 1). Now $E_{2n}(-2\Phi) = -E_{-2n}(2\Phi)$; also, $E_{-2n}(2\Phi) = E_{2n}(2\Phi)$ for integer values of n, and $J_{-2n}(2\Phi) = J_{2n}(2\Phi)$. Then equation (A4) becomes

$$V_n = J_{2n}(2\Phi) - iE_{2n}(2\Phi) \quad (A5)$$

Noting that $\Phi = \xi e^{i\pi/2}$, it is seen that

$$J_{2n}(2\Phi) = (-1)^n I_{2n}(2\xi) \quad (A6)$$

where I_{2n} is the modified Bessel function of the first kind From reference 1, for n an integer,

$$E_{2n}(2\Phi) = \begin{cases} -H_0(2\Phi), & n = 0 \\ \dfrac{1}{\pi}\displaystyle\sum_{k=0}^{n-1} \dfrac{\Gamma\left(k + \frac{1}{2}\right)\Phi^{2n-2k-1}}{\Gamma\left(2n + \frac{1}{2} - k\right)} - H_{2n}(2\Phi), & n \geq 1 \end{cases}$$

where H_{2n} is the Struve function. Making the change of variable gives

$$E_{2n}(2\xi e^{i\pi/2}) = \begin{cases} -iL_0(2\xi), & n = 0 \\ i(-1)^{n+1}\left[L_{2n}(2\xi) + \dfrac{1}{\pi}\displaystyle\sum_{k=0}^{n-1} \dfrac{k\Gamma\left(k + \frac{1}{2}\right)\xi^{2n-2k-1}}{\Gamma\left(2n + \frac{1}{2} - k\right)}\right], & n \geq 1 \end{cases} \tag{A7}$$

where L_{2n} is the modified Struve function (see reference 1).

Substitution of (A6) and (A7) into (A5) gives

$$V_n(\xi) = (-1)^n\left[I_{2n}(2\xi) - L_{2n}(2\xi) - \frac{1}{\pi}\sum_{k=0}^{n-1}(-1)\frac{k\Gamma\left(k + \frac{1}{2}\right)\xi^{2n-2k-1}}{\Gamma\left(2n + \frac{1}{2} - k\right)}\right] \tag{A8}$$

where the finite sum is to be omitted for $n = 0$.

APPENDIX B

STRESS CONCENTRATION FACTORS FOR TWO EQUAL-LENGTH COLLINEAR CUTS

In this appendix attention is restricted to problems in which the two collinear cuts are of equal length. This restriction is effected by setting q equal to s in equations (11) and (12), which yields

$$\left.\begin{aligned} P_n(\xi) &= 1 + \sum_{i=-(m+s)}^{-(m+1)} N_{n-1}(\xi)U_1(0) + \sum_{i=r+1}^{r+s} N_{n-i}(\xi)U_i(0) \\ U_n(\xi) &= \xi + \sum_{i=-(m+s)}^{-(m+1)} V_{n-1}(\xi)U_1(0) + \sum_{i=r+1}^{r+s} V_{n-1}(\xi)U_1(0) \end{aligned}\right\} \tag{B1}$$

and

$$0 = 1 + \sum_{i=-(m+s)}^{-(m+1)} N_{n-i}(0)U_1(0) + \sum_{i=r+1}^{r+s} N_{n-i}(0)U_1(0),$$

$$(m+s) \leq n \leq -(m+1), \qquad r+1 \leq n \leq r+s \tag{B2}$$

One of two cases arises, depending on whether the number of intact filaments between the cuts (interior filaments) is odd or even. The case of an odd number of interior filaments is treated first.

Odd number of interior filaments.- When the two cuts are of equal length, the displacements are symmetric with respect to the line which

equally divides the group of interior filaments. In this case it is convenient to take the zeroth filament as the line of symmetry, so that $m = r$ in equations (B1) and (B2), and the total number of interior filaments is $2r + 1$. With $U_1(0) = U_{-1}(0)$ because of symmetry, equations (B1) and (B2) become after some manipulation

$$\left.\begin{aligned} P_n(\xi) &= 1 + \sum_{i=r+1}^{r+s} \left\{ N_{n+i}(\xi) + N_{n-i}(\xi) \right\} U_i(0) \\ U_n(\xi) &= \quad + \sum_{i=r+1}^{r+s} \left\{ V_{n+i}(\xi) + V_{n-i}(\xi) \right\} U_i(0) \end{aligned}\right\} \tag{B3}$$

and

$$0 = 1 + \sum_{i=r+1}^{r+s} \left\{ N_{n+i}(0) + N_{n-i}(0) \right\} U_i(0), \qquad r + 1 \leq n \leq r + s \tag{B4}$$

The maximum load will occur adjacent to the cuts ($\xi = 0$) in the two outermost interior filaments ($n = \pm r$). Hence, from the first of equations (B3), the stress concentration factor for two cuts across s filaments separated by $2r + 1$ filaments is

$$K_{s,2r+1} = P_r(0) = 1 + \sum_{i=r+1}^{r+s} \left\{ N_{r+i}(0) + N_{r-i}(0) \right\} U_i(0) \tag{B5}$$

where the $U_i(0)$'s are calculated from equation (B4) for specified values of r and s.

Even number of interior filaments.- In this case, the interior filaments are assumed to be identified by $-m \leqq n \leqq r$, which with $r = m - 1$ becomes $-m \leqq n \leqq m - 1$. Equations (B1) and (B2) take the form

$$\left.\begin{aligned} P_n(\xi) &= 1 + \sum_{i=-(m+s)}^{-(m+1)} N_{n-i}(\xi)U_i(0) + \sum_{i=m}^{m+s-1} N_{n-i}(\xi)U_i(0) \\ U_n(\xi) &= \xi + \sum_{i=-(m+s)}^{-(m+1)} V_{n-i}(\xi)U_i(0) + \sum_{i=m}^{m+s-1} V_{n-i}(\xi)U_i(0) \end{aligned}\right\} \tag{B6}$$

and

$$0 = 1 + \sum_{i=-(m+s)}^{-(m+1)} N_{n-i}(0)U_i(0) + \sum_{i=m}^{m+s-1} N_{n-i}(0)U_i(0),$$

$$-(m+s) \leqq n \leqq -(m+1), \qquad m \leqq n \leqq m+s-1 \tag{B7}$$

For this configuration, the axial line of symmetry is located between the filaments numbered 0 and -1, which means that

$$U_{-i}(0) = U_{i-1}(0) \tag{B8}$$

After substitution from equation (B8) and some manipulation, equations (B6) and (B7) become

$$\left.\begin{aligned} P_n(\xi) &= 1 + \sum_{\imath=r}^{r+s-1} \left\{ N_{n+\imath+1}(\xi) + N_{n-\imath}(\xi) \right\} U_\imath(0) \\ U_n(\xi) &= \xi + \sum_{\imath=r}^{r+s-1} \left\{ V_{n+\imath+1}(\xi) + V_{n-\imath}(\xi) \right\} U_\imath(0) \end{aligned}\right\} \tag{B9}$$

and

$$0 = 1 + \sum_{\imath=r}^{r+s-1} \left\{ N_{n+\imath+1}(0) + N_{n-\imath}(0) \right\} U_\imath(0), \qquad r \leq n \leq r + s - 1 \tag{B10}$$

In this case the maximum load occurs for $n = -r,\ r - 1$. Then with $n = r - 1$ in the first of equations (B9), the stress concentration factor for two cuts across s filaments, separated by $2r$ filaments, is

$$K_{s,2r} = P_{r-1}(0) = 1 + \sum_{i=r}^{r+s-1} \left\{ N_{r+\imath}(0) + N_{r-\imath-1}(0) \right\} U_\imath(0) \tag{B11}$$

where the $U_\imath(0)$'s are calculated from equations (B10) for specified values of r and s.

APPENDIX C

GENERAL PROOF OF FORMULA (26)*

From the system of linear algebraic equations

$$\sum_{r=0}^{n-1} N_{i-r}(0)U_r(0) = -1, \quad 0 \leq i \leq n-1 \tag{C1}$$

it is desired to obtain an expression for $U_0(0)$ which is valid for all positive values of n. It is convenient to let

$$W_r = \frac{4}{\pi} U_r(0)$$

$$H_k(0) = \frac{\pi}{4} N_k(0) = \frac{1}{2}\left(\frac{1}{2k-1} - \frac{1}{2k+1}\right)$$

and

$$m = n - 1$$

Then the system (C1) becomes

$$\sum_{k=0}^{m} H_{i-k}(0)W_k = -1, \quad 0 \leq i \leq m$$

---

*Communicated to the author by W. J. Harrington, Professor of Mathematics, North Carolina State University.

or, in an equivalent form

$$\left\{\begin{array}{l} (-1-1)W_0 + \left(1 - \frac{1}{3}\right)W_1 + \ldots + \left(\frac{1}{2m-1} - \frac{1}{2m+1}\right)W_m = -2 \\ \left(1 - \frac{1}{3}\right)W_0 + (-1-1)W_1 + \ldots + \left(\frac{1}{2m-3} - \frac{1}{2m-1}\right)W_m = -2 \\ \ldots\ldots\ldots\ldots\ldots\ldots\ldots\ldots\ldots\ldots\ldots\ldots \\ \left(\frac{1}{2m-3} - \frac{1}{2m-1}\right)W_0 + \ldots + (-1-1)W_{m-1} + \left(1 - \frac{1}{3}\right)W_m = -2 \\ \left(\frac{1}{2m-1} - \frac{1}{2m+1}\right)W_0 + \ldots + \left(1 - \frac{1}{3}\right)W_{m-1} + (-1-1)W_m = -2 \end{array}\right\} \quad (C2)$$

The system (C2) can be replaced by a new system composed of the equations of (C2) linearly combined in the following manner:

(1) First equation multiplied by $(-\frac{1}{2})$;

(2) Sum of first two equations multiplied by $(-\frac{1}{4})$;

(3) Sum of first three equations multiplied by $(-\frac{1}{6})$;

(m+1). Sum of first (m+1) equations multiplied by $(-\frac{1}{2m+2})$. Now let $w_k = \frac{W_k}{2k+1}$, and the new system has the form

$$\underline{A}\,\underline{w} \equiv \begin{bmatrix} 1 & -1 & -\frac{1}{3} & -\frac{1}{5} & \cdots & \frac{1}{2m-1} \\ \frac{1}{3} & 1 & -1 & -\frac{1}{3} & \cdots & \frac{1}{2m-3} \\ \frac{1}{5} & \frac{1}{3} & 1 & -1 & \cdots & \frac{1}{2m-5} \\ \cdots & \cdots & \cdots & \cdots & \cdots & \cdots \\ \frac{1}{2m-1} & \frac{1}{2m-3} & \cdots & \cdots & 1 & -1 \\ \frac{1}{2m+1} & \frac{1}{2m-1} & \cdots & \cdots & \frac{1}{3} & 1 \end{bmatrix} \begin{bmatrix} w_0 \\ w_1 \\ w_2 \\ \cdots \\ w_{m-1} \\ w_m \end{bmatrix} = \begin{bmatrix} 1 \\ 1 \\ 1 \\ \cdots \\ 1 \\ 1 \end{bmatrix} \tag{C3}$$

The object is to calculate w_0. To this end it would be advantageous to have a row vector which is orthogonal to all column vectors of the matrix $\underline{A}$ except the first. On page 102 of reference 7 is given the identity

$$G_1(m) \equiv \sum_{k=0}^{m} \binom{2k}{k}\binom{2m-2k}{m-k}\frac{1}{2m-2k-1}$$

$$= \sum_{k=0}^{m} \binom{2k}{k}\binom{2m-2k}{m-k}\frac{1}{2k-1} = -\delta_{m0} \tag{C4}$$

where δ_{m0} is the Kronecker delta. With $m \geqq 1$ (i.e., $n \geqq 2$), this provides a row vector,

$$\left[\binom{2m}{m}, \binom{2}{1}\binom{2m-2}{m-1}, \ldots, \binom{2}{1}\binom{2m-2}{m-1}, \binom{2m}{m}\right] \tag{C5}$$

which is orthogonal to the second column of the matrix $\underline{A}$. It can be shown that this vector is orthogonal to all the columns of $\underline{A}$ except the first. The proof is by induction By way of example, it will be shown that the identity (C4) implies that

$$G_3(m) \equiv \sum_{k=0}^{m} \binom{2k}{k}\binom{2m-2k}{m-k}\frac{1}{2k-3} = 0 \quad \text{if} \quad m \geq 2 \tag{C6}$$

Equation (C6) can be written

$$G_3(m) = -\frac{1}{3}\binom{2m}{m} + \sum_{k=0}^{m-1} \frac{\binom{2k+2}{k+1}\binom{2m-2k-2}{m-k-1}}{2k-1} \tag{C7}$$

Also,

$$\binom{2k+2}{k+1} = 2\binom{2k}{k} + 2\binom{2k}{k+1}$$

$$= 4\binom{2k}{k} - 2\binom{2k}{k}\cdot\frac{1}{k+1}$$

Thus

$$\frac{\binom{2k+2}{2k+1}}{2k-1} = \frac{4\binom{2k}{k}}{2k-1} - \frac{2\binom{2k}{k}}{(2k-1)(k+1)}$$

$$= \frac{8}{3}\frac{\binom{2k}{k}}{2k-1} + \frac{2}{3}\frac{\binom{2k}{k}}{k+1}$$

Therefore, (C7) becomes

$$G_3(m) = -\frac{1}{3}\binom{2m}{m} + \frac{8}{3}G_1(m-1) + \frac{2}{3}\sum_{k=0}^{m-1}\binom{2k}{k}\binom{2m-2k-2}{m-k-1}\cdot\frac{1}{k+1} \qquad (C8)$$

On page 121 of reference 7, problem 11(a), appears an identity such that

$$\sum_{k=0}^{n}\binom{2k}{k}\binom{2n-2k}{n-k}\frac{1}{k+1} = \frac{1}{2}\binom{2n+2}{n+1} \qquad (C9)$$

Thus if $m > 1$, then $G_1(m-1) = 0$, and from (C8) and (C9) there results

$$G_3(m) = -\frac{1}{3}\binom{2m}{m} + \frac{2}{3}\cdot\frac{1}{2}\binom{2m}{m} = 0, \quad m \geq 1$$

Similar results can be obtained for $G_5(m)$, $G_7(m)$, etc., from which the pattern of the induction proof can be recognized.

Thus, for each $m \geq 1$, the row vector (C5) is orthogonal to all column vectors of the matrix $\underline{A}$ except the first. Premultiplication of (C3) by the row vector (C5) yields

$$\left[\sum_{k=0}^{m}\binom{2k}{k}\binom{2m-2k}{m-k}\cdot\frac{1}{2k+1}\right]\cdot w_0 = \sum_{k=0}^{m}\binom{2k}{k}\binom{2m-2k}{m-k} \qquad (C10)$$

In problem 10(a), page 121, of reference 7, the summation on the left-hand side of (C10) is evaluated; the result is

$$\sum_{k=0}^{m} \binom{2k}{k}\binom{2m-2k}{m-k}\frac{1}{2k+1} = \frac{2^{4m}}{(2m+1)\binom{2m}{m}} = \frac{2^{4m}(m!)^2}{(2m+1)!} \tag{C11}$$

Also, on page 130 of reference 7 the right-hand side of (C10) is evaluated as

$$\sum_{k=0}^{m} \binom{2k}{k}\binom{2m-2k}{m-k} = 2^{2m} \tag{C12}$$

By use of (C11) and (C12), the solution to equation (C10) is found to be

$$w_o = \frac{4}{\pi} U_0(0) = \frac{(2m+1)!}{2^{2m}(m!)^2}$$

or, replacing m by n - 1,

$$\frac{4}{\pi} U_0(0) = \frac{(2n-1)!}{2^{2n-2}\left[(n-1)!\right]^2}, \quad n = 1,2,3, \ldots$$

which is equivalent to equation (26).

APPENDIX D

SUMMATION OF THE INFINITE SERIES $\sum_{k=-\infty}^{\infty} N_{Rk+j}(0)$

The infinite series to be summed is given by

$$\lambda(R,J) = \sum_{k=-\infty}^{\infty} N_{Rk+J}(0) \tag{D1}$$

where $N_{Rk+J}(0)$ is given by

$$N_{Rk+j}(0) = \frac{4}{\pi\left\{4(Rk + J)^2 - 1\right\}}$$

and where R is a positive integer, k is an integer, and j is an integer such that $R > J$. Then equation (D1) can be written as

$$\lambda(R,j) = \frac{4}{\pi}\sum_{k=-\infty}^{\infty} \frac{1}{4(Rk + J)^2 - 1}$$

which can be changed to

$$\lambda(R,J) = \frac{1}{\pi R^2} \sum_{k=-\infty}^{\infty} \frac{1}{\left\{k + \frac{1}{R}\left(J - \frac{1}{2}\right)\right\}\left\{k + \frac{1}{R}\left(j + \frac{1}{2}\right)\right\}} \tag{D2}$$

Therefore the problem is equivalent to summing the series

$$\varphi(\alpha,\beta) = \sum_{k=-\infty}^{\infty}{}' \frac{1}{(k-\alpha)(k-\beta)} \tag{D3}$$

where $\alpha = -\frac{1}{R}\left(j - \frac{1}{2}\right)$, $\beta = -\frac{1}{R}\left(j + \frac{1}{2}\right)$; α and β not integers.

The problem is amenable to a method presented in reference 2. We investigate the contour integral

$$B_q = \int_{C_q} \frac{\pi \cot \pi z}{(z-\alpha)(z-\beta)}\, dz \tag{D4}$$

where C_q is the square contour with corners at $z = \left(q + \frac{1}{2}\right)e^{i\pi(2m+1)/4}$, where $m = 1, 2, 3,$ and 4, and q is a positive integer. The presence of $\cot \pi z$ in the integrand of (B4) provides a pole at each integer value of z. On each side of the contour $\cot \pi z$ is bounded, so that $\lim_{q\to\infty} B_q = 0$. Calculation of residues at the poles enclosed by the contour then yields

$$\lim_{q\to\infty} B_q = \pi\left(\frac{\cot \pi\alpha}{\alpha - \beta} + \frac{\cot \pi\beta}{\beta - \alpha}\right) + \sum_{k=-\infty}^{\infty} \frac{1}{(k-\alpha)(k-\beta)} = 0$$

so that

$$\sum_{k=-\infty}^{\infty}{}' \frac{1}{(k-\alpha)(k-\beta)} = \frac{\pi}{\alpha - \beta}(\cot \pi\beta - \cot \pi\alpha) \tag{D5}$$

Substitution of (C5) into (C2), noting that $\alpha = -\frac{1}{R}\left(J - \frac{1}{2}\right)$ and $\beta = -\frac{1}{R}\left(J + \frac{1}{2}\right)$, yields

$$\lambda(R,J) = \frac{1}{\pi R^2}(\pi R)\left\{\cot\frac{\pi}{R}\left(J - \frac{1}{2}\right) - \cot\frac{\pi}{R}\left(J + \frac{1}{2}\right)\right\}$$

or

$$\sum_{k=-\infty}^{\infty} N_{Rk+j}(0) = \frac{1}{R}\left\{\cot\frac{\pi}{R}\left(j - \frac{1}{2}\right) - \cot\frac{\pi}{R}\left(j + \frac{1}{2}\right)\right\}$$

APPENDIX E

CALCULATION OF DYNAMIC STRESS CONCENTRATION FACTORS

In dimensionless form the governing equations are

Conservation of momentum:

$$\frac{\partial^2 U_n}{\partial \xi^2} + U_{n+1} - 2U_n + U_{n-1} = \frac{\partial^2 U_n}{\partial \tau^2} \tag{E1}$$

Boundary conditions:

$$U_n(0,\tau) = 0, \qquad -m \leqq n \leqq r, \qquad -(m+q+1) \geqq n, \qquad n \geqq r+s+1$$

$$P_n(0,\tau) = 0, \qquad -(m+q) \leqq n \leqq -(m+1), \qquad r+1 \leqq n \leqq r+s \tag{E2}$$

$$P(\pm\infty,\tau) = 1 \tag{E3}$$

Initial conditions:

$$P_n(\xi,0) = 1$$

$$\frac{\partial U_n}{\partial \tau}(\xi,0) = 0 \tag{E4}$$

Application of the Laplace transform to equations (E1) to (E3) and use of equations (E4) yield

$$\frac{\partial^2 U_n^*}{\partial \xi^2} + U_{n+1}^* - (2+\zeta^2)U_n^* + U_{n-1}^* = -\zeta\xi \tag{E5}$$

with

$$U_n^*(0,\zeta) = 0, \qquad -m \leqq n \leqq r, \qquad -(m+q) \geqq n, \qquad n \geqq r+s+1$$

$$P_n^*(0,\zeta) = 0, \qquad -(m+q) \leqq n \leqq -(m+1), \qquad r+1 \leqq n \leqq r+s \tag{E6}$$

$$\frac{\partial U_n^*}{\partial \xi}(\pm\infty,\zeta) = \frac{1}{\zeta}$$

where the first of equations (E4) has been converted to the condition $U_n(\xi,0) = \xi$, and the asterisks denote transformed quantities.

Following the procedure of reference 4, use can be made of the unit solution to write the transformed loads and displacements in the form

$$P_n^*(\xi,\zeta) = \frac{1}{\zeta} + \sum_{i=-(m+q)}^{-(m+1)} N_{n-i}^*(\xi,\zeta)U_i^*(0,\zeta) + \sum_{i=r+1}^{r+s} N_{n-i}^*(\xi,\zeta)U_i^*(0,\zeta) \tag{E7}$$

$$U_n^*(\xi,\zeta) = \frac{\xi}{\zeta} + \sum_{i=-(m+q)}^{-(m+1)} V_{n-i}^*(\xi,\zeta)U_i^*(0,\zeta) + \sum_{i=r+1}^{r+s} V_{n-i}^*(\xi,\zeta)U_i^*(0,\zeta) \tag{E8}$$

with the remaining boundary conditions (E6) taking the form

$$0 = \frac{1}{\zeta} + \sum_{i=-(m+q)}^{-(m+1)} N^*_{n-1}(0,\zeta)U^*_i(0,\zeta)$$

$$+ \sum_{i=r+1}^{r+s} N^*_{n-i}(0,\zeta)U^*_1(0,\zeta), \qquad \begin{matrix} -(m+q) \leqq n \leqq -(m+1), \\ r+1 \leqq n \leqq r+s \end{matrix} \qquad \text{(E9)}$$

Here the investigation is restricted to the cases of two equal-length collinear cuts separated by a single intact filament, which for convenience is taken to be the zeroeth filament. Thus, with $m = r = 0$, $q = s$, and symmetry of displacements accounted for, equations (E7) and (E9) become

$$P^*_n(\xi,\zeta) = \frac{1}{\zeta} + \sum_{i=1}^{s} \left\{N^*_{n+1}(\xi,\zeta) + N^*_{n-1}(\xi,\zeta)\right\}U^*_1(0,\zeta) \qquad \text{(E10)}$$

and

$$0 = \frac{1}{\zeta} + \sum_{i=1}^{s} \left\{N^*_1(0,\zeta) + N^*_{-1}(0,\zeta)\right\}U^*_i(0,\zeta), \qquad 1 \leqq n \leqq s \qquad \text{(E11)}$$

so that the cuts are separated by the zeroeth filament, and each cut severs s filaments. The transformed load in the zeroeth filament, which is the most highly stressed, is given by

$$P^*_o(\xi,\zeta) = \frac{1}{\zeta} + \sum_{i=1}^{s} \left\{N^*_1(\xi,\zeta) + N^*_{-1}(\xi,\zeta)\right\}U^*_i(0,\zeta) \qquad \text{(E12)}$$

The stress concentration factor is the maximum value of this load, which occurs at $\xi = 0$. Hence, the transformed stress concentration factor for two cuts across n filaments and separated by a single intact filament is given by

$$K^*_{n,1}(\zeta) = P^*_o(0,\zeta) = \frac{1}{\zeta} + \sum_{i=1}^{n} \left\{ N^*_i(0,\zeta) + N^*_{-i}(0,\zeta) \right\} U^*_i(0,\zeta) \qquad \text{(E13)}$$

The transformed influence function was found in reference 4 to be

$$N^*_m(0,\zeta) = -\frac{1}{\pi} \int_0^{\pi} \cos m\theta \sqrt{4 \sin^2 \frac{\theta}{2} + \zeta^2}\, d\theta \qquad \text{(E14)}$$

From equation (E14) it can be seen that $N^*_m(0,\zeta) = N^*_{-m}(0,\zeta)$, so that equations (E13) and (E11) can be written as

$$K^*_{n,1}(\zeta) = \frac{1}{\zeta} + 2 \sum_{i=1}^{n} N^*_i(0,\zeta) U^*_i(0,\zeta) \qquad \text{(E15)}$$

and

$$0 = \frac{1}{\zeta} + \sum_{i=1}^{n} \left\{ N^*_{r+i}(0,\zeta) + N^*_{r+1}(0,\zeta) \right\} U^*_1(0,\zeta), \qquad 1 \leq r \leq n \qquad \text{(E16)}$$

For the cases in which each cut is across one and two filaments, solution of equations (E16) for $n = 1$ and $n = 2$ yields

$$K^*_{1,1}(\zeta) = \frac{1}{\zeta} \left\{ 1 - \frac{2N^*_1}{N^*_0 + N^*_2} \right\} \qquad \text{(E17)}$$

and

$$K^*_{2,1}(\zeta) = \frac{1}{\zeta}\left[1 - 2\left\{\frac{N^*_1(N^*_0 + N^*_4) + N^*_2(N^*_0 + N^*_2) - (N^*_1 + N^*_2)(N^*_1 + N^*_3)}{(N^*_0 + N^*_2)(N^*_0 + N^*_4) - (N^*_1 + N^*_3)^2}\right\}\right] \quad \text{(E18)}$$

where, for brevity, the functional dependence of the transformed influence functions has been omitted.

The inversion integral for the stress concentration factor is

$$K_{n,1}(\tau) = \frac{1}{2\pi i}\int_{\epsilon-i\infty}^{\epsilon+i\infty} K^*_{n,1}(\zeta)e^{\zeta\tau}\,d\zeta \quad \text{(E19)}$$

A series evaluation of this integral can be made by use of the method employed in reference 4 for the single-cut problem. Briefly, the method employs a conformal mapping function given by $\zeta = z - 1/z$ to transform the inversion integral (E19) into an integral around a contour C just inside the unit circle in the z-plane, given by

$$K_{n,1}(\tau) = -\frac{1}{2\pi i}\oint_C \left[\zeta K^*_{n,1}\right]\frac{z^2 + 1}{z^2 - 1}\,e^{(z-1/z)\tau}\,\frac{dz}{z} \quad \text{(E20)}$$

This integral is evaluated by finding the coefficient of the zeroeth power of z in the expansion of

$$\left[\zeta K^*_{n,1}\right]\frac{z^2 + 1}{z^2 - 1}\,e^{(z-1/z)\tau} \quad \text{(E21)}$$

The term in brackets in (E21) can be expanded in a power series in z by using equation (E17) or (E18) in conjunction with the series expansion for $N_m^*(0,z)$, which was found in reference 4 to be

$$N_m(0,z) = -\frac{1}{z}\sum_{k=0}^{\infty}\binom{1/2}{k}\binom{1/2}{k+m}(-z^2)^{2k+m} \tag{E22}$$

where $\binom{1/2}{k}$ is the binomial number given by $\binom{1/2}{0} = 1$, and

$$\binom{1/2}{k} = \frac{\frac{1}{2}\left(\frac{1}{2}-1\right)\left(\frac{1}{2}-2\right)\cdots\left(\frac{1}{2}-k+1\right)}{k!}, \qquad k = 1,2,3, \ldots$$

Since the expansion for $\zeta K_{n,1}^*$ involves only positive even powers of z, only the negative even powers in the expansion of the other part of (E21) need be sought. It was found in reference 4 that if

$$\frac{z^2+1}{z^2-1}\,e^{(z-1/z)\tau} = \sum_{k=-\infty}^{\infty} C_k z^k$$

then

$$C_0 = -1$$

$$C_{-k} = J_0(2\tau) + 2J_2(2\tau) + \cdots 2J_{k-2}(2\tau) + J_k(2\tau) - 1, \tag{E23}$$

$$k = 2, 4, 6, \ldots$$

after considerable manipulation, the results are found to be

$$K_{1,1}(\tau) = 1 - C_2(\tau) + \frac{1}{4} C_6(\tau) + \frac{1}{32} C_{10}(\tau) - \frac{1}{2^9} C_{14}(\tau)$$

$$+ \frac{1}{2^9} C_{18}(\tau) + \frac{47}{2^{16}} C_{22}(\tau) + \cdots \qquad \text{(E24)}$$

and

$$K_{2,1}(\tau) = 1 - C_2(\tau) - \frac{3}{4} C_4(\tau) - \frac{1}{8} C_6(\tau) + \frac{3}{16} C_8(\tau) + \frac{11}{64} C_{10}(\tau)$$

$$+ \frac{15}{2^8} C_{12}(\tau) + \frac{49}{2^{10}} C_{14}(\tau) + \frac{81}{2^{11}} C_{16}(\tau) + \frac{47}{2^{12}} C_{18}(\tau)$$

$$- \frac{99}{2^{15}} C_{20}(\tau) - \frac{523}{2^{17}} C_{22}(\tau) + \cdots$$

Good convergence is obtained for the range of τ investigated.